Mechanosensitivity and Neural Adaptation in Human Somatosensory System.

by

Lalit Kumar Venkatesan

Submitted to the graduate degree program in Neurosciences and the Graduate Faculty of the University of Kansas in partial fulfillment of the requirements for the degree of Doctor of Philosophy.

Steven M. Barlow, PhD.
Committee Chairperson*

Paul D. Cheney, PhD.
Committee Member

Mihai Popescu, PhD.
Committee Member

John A. Stanford, PhD.
Committee Member

Jungwon J. Choy, PhD.
Committee Member

Date Defended: April 13, 2012

The Dissertation Committee for Lalit Kumar Venkatesan certifies
that this is the approved version of the following dissertation:

Mechanosensitivity and Neural Adaptation in Human Somatosensory System.

Steven M. Barlow, PhD.
Committee Chairperson*

Date Approved: April 13, 2012

ABSTRACT

Magnetoencephalography (MEG) was utilized to characterize the adaptation in the somatosensory cortical network due to repeated cutaneous tactile stimulation applied unilaterally on the face and hand using a custom-built pneumatic stimulator called the TAC-Cell. Face stimulation invoked neuromagnetic responses reflecting cortical activity in the contralateral primary somatosensory cortex (SI), while hand stimulation resulted in robust contralateral SI and posterior parietal cortex (PPC) activation. There was also activity observed in regions of the secondary somatosensory cortical areas (SII), although with a reduced amplitude and higher variability across subjects.

There was a significant difference in adaptation rates between SI, and higher-order sensory cortices like the PPC for hand stimulation. Adaptation was also significantly dependent on the stimulus frequency and pulse index number within the stimulus train for both hand and face stimulation. The latency of the peak responses was significantly dependent on stimulus site and response component (SI, PPC). The difference in the latency of peak SI and PPC responses can be reflective of a hierarchical serial-processing network in the somatosensory cortex.

Age- and sex-related changes of vibrotactile sensitivity in the orofacial and hand skin surfaces of healthy adults was demonstrated using an established psychophysical protocol. Vibrotactile threshold sensitivity increased as a function of age for finger stimulation, but remained unaltered for the face. Increase in the finger threshold sensitivity is due to age-related changes in the number and morphology of Pacinian corpuscles (absent in the face). Vibrotactile threshold sensitivity is significantly dependent on stimulation site, stimulus frequency, and sex of

the participant. These differences are presumably due to dissimilarities in the type and density of mechanoreceptors present in the face and hand.

A novel-method was developed to couple the use of fiber-optic displacement sensors with the pneumatic stimulator built in our laboratory called the TAC-Cell. This displacement sensor which is commonly used in industrial applications was successfully utilized to characterize the skin response to TAC-Cell stimulation. Skin displacement was significantly dependent on input stimulus amplitudes and varied as a function of the participants' sex. Power spectrum analysis and rise-fall time measurement of the skin-displacement showed that the TAC-Cell stimulus consists of a spectrally rich, high velocity signal that is capable of evoking a cortical response due to stimulation of the medial-lemniscus and trigeminal pathways.

ACKNOWLEDGEMENTS

This study was supported in part by NIH R01 DC003311 (Barlow), NIH P30 HD02528, and the Sutherland Family Foundation (Barlow). I would like to thank my advisor, Dr. Steven M. Barlow for his continual support and encouragement throughout my graduate program at the University of Kansas. From the time he hired me as an engineering graduate student, he has provided me plenty of opportunities to learn and develop skills that would help me to further my scientific career. I would like to thank my dissertation committee members: Dr. Paul Cheney, Dr. Mihai Popescu, Dr. John Stanford, and Dr. Janet Choy for their support throughout my dissertation research.

I would especially like to thank Dr. Mihai Popescu and Dr. Anda Popescu of the Hoglund Brain Imaging Center (HBIC) at KUMED for helping me with the collection of MEG data, and also for spending the time to teach me the neuroimaging data processing and analysis methods. A special thanks to Allan Schmitt, MRI Laboratory Director at HBIC for assistance with scheduling experiments and MRI data collection.

I want to thank Doug Kieweg, DEEC project coordinator for developing the software for the *VIBROS* experiment, and for taking the time to teach me LabVIEW programming when I was with DEEC. I want to also thank Joan Wang, engineer at Communication Neuroscience Laboratories (CNL) assistance in software design and data analysis.

I would like to thank all current and past members of the CNL. You made graduate school more enjoyable.

I would like to thank my mother, grandparents, and brother for encouraging me throughout my life. Without you folks, none of this would have happened. I would like to thank my wife Meghann, and son Sanjay for being patient with me, and for being a source of support and encouragement. They made it all worth it.

TABLE OF CONTENTS

LIST OF FIGURES

LIST OF TABLES

ABBREVIATION KEY

Brodmann's area…….. ....(BA)

Electrooculogram……. ...(EOG)

Fast-Adapting……...….....(FA)

Independent Component……..……....(IC)

Magnetoencephalography……... …(MEG)

Non-Pacinian…….....(NP)

Pacinian…… ...(P)

Parietal ventral…….(PV)

Posterior parietal cortex ……..(PPC)

Primary somatosensory cortex……. ...(SI)

Somatosensory evoked field……(SEF)

Secondary somatosensory cortex…….(SII)

Single-interval up/down……. …….(SIUD)

Slow-Adapting…….……(SA)

Vibrotactile Detection Threshold…… (VDT)

CHAPTER ONE: INTRODUCTION

The ability to adapt to intrinsic changes (e.g., growth in body plan, viscoelastic properties of connective and contractile tissues, aging) and/or extrinsic conditions (e.g., task dynamics [load, direction, active stiffness] or imposed perturbations [environment]) is one of the fundamental functions of the human nervous system. Adaptation and integration of signals from different modalities and different sections of the brain are essential for normal sensorimotor function. Cortical adaptation in sensory systems (visual, auditory, olfactory, and somatosensory) is commonly studied using different stimulus modalities and recording techniques. Despite evidence that somatosensory adaptation plays significant role in sensory function, no attempt has been made to investigate the adaptation patterns in different regions of the human somatosensory cortical network in response to highly controlled pneumatic inputs to cutaneous skin. The principal cortical network involved in somatosensory processing includes the primary somatosensory cortex (SI), the secondary somatosensory cortex (SII), and somatosensory association areas like the posterior parietal cortex (PPC).

Functional magnetoencephalography (MEG) will be used in healthy adults to improve our knowledge of the adaptation processes in areas of the somatosensory cortical network (SI, SII, and PPC) during cutaneous stimulation of the hand and face. This part of the study (Aim 1) will be carried out in a group of young neurotypical adults to establish feasibility and demonstrate the effectiveness of these stimulation paradigms prior to conducting future studies in the elderly.

Our long-term goal is to develop advanced neurological testing techniques and therapeutic treatments using the TAC-Cell for patients who have suffered cerebrovascular stroke /traumatic brain injury or in pediatric populations with sensorimotor integrative disorders

affecting attention (autism) and speech-language development. Incidence of brain injury and progressive neurological disease increases with age, and sense of touch is altered in elderly (Gescheider et al., 1996; Stevens and Choo, 1996; Stevens and Cruz, 1996). The loss of tactile sensation is partly attributed to the decreases in sensory nerve function and epidermal innervation (Khalil et al., 1994; Lauria et al., 1999). Healthy aging is accompanied by metabolic, structural, and physiological changes in the brain that can affect the transmission of tactile information. However, our knowledge of age-related changes in the perceptual response is limited. This information would enable us to develop better diagnosis and treatment design for neurological disorders and diseases that are common in older adults. Thus, Aim 2 will utilize an established psychophysical protocol to study age- and sex-related changes in face and hand skin vibrotactile sensitivity in a healthy group of adults. For future studies, it is essential to understand the characteristics of the TAC-Cell stimulus when presented to skin. In Aim 3, we use a novel- design where we adapt a fiber-optic sensor to measure skin displacement due to TAC-Cell stimulation. This will help increase our understanding of the differences in male and female skin displacement amplitudes for different TAC-Cell stimulus inputs. This will also help us to quantify stimulus characteristics like stimulus pressure, rise-fall times, and power spectra for different TAC-Cell inputs.

SPECIFIC AIM #1

Characterize adaptation and latency of the response of the somatosensory cortical network to repetitive stimulation at a single site of the hand and face

Using MEG recordings among a group of healthy adults (age 18 to 30 years), we will characterize and compare:

• 1a. The SI, SII, and PPC adaptation for hand (glabrous surface of distal phalanx of right index finger), and face (right non-glabrous surface of the oral angle) stimulation as a function of stimulus frequency (2Hz, 4Hz);

• 1b. The SI, SII, and PPC peak dipole *latency* as a function of stimulus site (hand – glabrous surface of distal phalanx of right index finger, face – right non-glabrous surface of the oral angle).

SPECIFIC AIM #2

Vibrotactile detection threshold assessment for hand and face

To test the age-related changes in cutaneous vibrotactile sensitivity thresholds of the face and hand among a group of healthy adults, we will determine:

• 2a. The differences in the vibrotactile detection thresholds (at 5, 10, 50, 150, 250, and 300 Hz) as a function of age among two groups, including younger adults: ages 18 to 30 years, and older adults: ages 58 to 70 years, and sex;

• 2b. The differences in the vibrotactile detection thresholds (at 5, 10, 50, 150, 250, and 300 Hz) as a function of skin site (hand – distal phalanx of right index finger, face – right lower lip vermilion, and right non-glabrous surface of oral angle).

SPECIFIC AIM #3

Characterize the TAC-Cell stimulus

A non-contact fiber-optic displacement sensor was used in healthy younger adults (ages 18 to 30 years) to characterize skin displacement for different stimulus inputs as a function of the participants' sex. In addition, stimulus pressure, rise-fall times, and power spectrum of skin displacement was measured and characterized.

BACKGROUND, SIGNIFICANCE, AND RATIONALE

ADAPTATION

Adaptation is a widely observed phenomenon at multiple levels of processing among all sensory channels of the nervous system (Hellweg et al., 1977; Ohzawa et al., 1982; Wilson, 1998). Acting over a range of time scales, adaptation has been implicated in both shifting the sensitivity of the system to maximize the dynamic range of encoding and priming the system for responses to novel stimuli (Abbott et al., 1997; Fairhall et al., 2001; Muller et al., 1999). Adaptation to changes in the stimulus properties is essential for efficient neural coding (Smirnakis et al., 1997). Adaptation solves the central problem of encoding a wide range of signals compared to limited responses available to the neuron. The sensory system adapts its input/output relation to the statistical properties of the dynamic changes in the environment, thus optimizing information transmission (Brenner et al., 2000).

Adaptation is a dynamic process reflected by a decrease in neuronal sensitivity due to repeated or sustained sensory stimulation, which can span a wide range of temporal scales ranging from milliseconds to the lifespan of an organism. Attenuation of sensory responses due to adaptation is a common mechanism in sensory systems (visual, auditory, olfactory and somatosensory), which is stimulus specific (since it depends on factors like stimulus strength and frequency), and generally more pronounced at cortical rather than subcortical levels (Chung et al., 2002).

Adaptation and consequent recovery depends on the time scale of stimulation. Brief stimulation results in rapid recovery whereas prolonged stimulation results in slower and more lasting forms of adaptation. In general, short-term adaptation leads to a rapid decay in the system response within the first few hundred milliseconds of stimulation, and this response is

substantially lower in amplitude than the activity observed at stimulus onset. Synaptic mechanisms underlying short-term adaptation depend on rapid neurotransmission processes like AMPA and NMDA receptor mediated excitatory neurotransmission, and $GABA_A$ receptor mediated inhibitory transmission. Long-term adaptation occurs as an outcome of continuous stimulation over a relatively long period of time (minutes, hours, or days) leading to plasticity and substantial changes in the network connectivity. These alterations are a product of changes in synaptic efficacy and axonal sprouting.

Central integration and processing of sensory inputs may rely on certain forms of neural architecture. For example, the existence of a rate-of-change network has been described that anticipates synaptic inputs from sensory systems and adjusts motor outputs accordingly (Puccini et al., 2007). Repetitive stimulation paradigms have shown that ongoing sensory inputs drive the sensory pathways in an adapted state, with dynamically evolving interplays between excitatory and inhibitory subpopulations of neurons that enhance sensory performance according to the dynamic range of the sensory input (Gabernet et al., 2005; Heiss et al., 2008; Higley and Contreras, 2006). Adaptation enhances intensity and frequency discrimination of supraliminal vibrotactile stimuli (Goble and Hollins, 1993; Goble and Hollins, 1994), and spatial localization of a subsequent stimulus (Tannan et al., 2006). Adaptation is useful in facilitating motor learning purely through perception and not motor training (Meegan et al., 2000). Adaptation is also crucial in developing systems to enable learning of new motor skills and in systems undergoing rehabilitation to relearn some of motor skills lost due to brain injury or stroke.

PRIMARY SOMATOSENSORY CORTEX (SI)

SI contains four areas, Brodmann's area (BA) 3a, 3b, 1, and 2. Areas 1, 2, and 3 are densely interconnected to the precentral motor cortex, the posterior parietal association cortex, SII, and the supplementary motor area (Jones and Powell, 1969a; Jones and Powell, 1969b; Jones and Powell, 1970a; Jones and Powell, 1970b). Areas 3a and 3b have denser thalamic innervations when compared to BA's 1 and 2. Cutaneous information from mechanoreceptors is processed in areas 3b and 1. Proprioceptive information from muscles, tendons and joints is processed in area 3a. Area 2 is thought to integrate the cutaneous and proprioceptive inputs (Hsiao, 2008). Extensive interconnections between these four SI areas enable the higher-order integration of sensory information. Functional mapping of the human SI using fMRI (Maldjian et al., 1999), and MEG (Hari et al., 1993; Nakamura et al., 1998) has confirmed the presence of medial to lateral representation of the foot, trunk, hand, lips and tongue.

Anatomical tracing studies (Padberg et al., 2009; Rausell et al., 1998) have demonstrated that the somatosensory system is characterized by a high degree of convergence and divergence of thalamocortical connections to SI, which confers unique processing features that make it more susceptible than other sensory systems (e.g. visual, auditory) to associative learning and plasticity (Jenkins et al., 1990; Xerri et al., 1998). This complex structural architecture seemingly sub-serves the major role of supporting a dynamic interaction with the environment. Voluntary motor activity in humans requires continuous sensory feedback (Pantano et al., 1995; Seitz et al., 1995), which implies that relevant tactile and proprioceptive information is extracted or integrated from/across a complex array of concurrent and dynamically changing afferent inputs to support the planning and execution of specific sequences of movements that involve functionally related body parts. Predicting the future state of the motor system is essential for

fine motor control because of the inherent delays in the sensorimotor system (Davidson and Wolpert, 2005). It has been suggested that the sensorimotor system uses an internal-forward model (Wolpert and Miall, 1996; Wolpert, 1997) to determine the sensory consequences of movement. An efference copy (Von Holst, 1954) of an outgoing motor command predicts the corresponding sensory outcome (corollary discharge) (Sperry, 1950), which is compared to the actual sensory feedback. The system compensates for this discrepancy for precise completion of the desired motor task.

SECONDARY SOMATOSENSORY CORTEX (SII)

SII is located in the parietal operculum, that is, the upper bank of the Sylvian fissure. The SII response is amplified during finger movements (Huttunen et al., 1996) and hand muscle contractions (Forss and Jousmaki, 1998), and it is suggested that this enhanced activation reflects an increase in the processing of tactile inputs during movement. Previous MEG studies have shown that the latency of the SII response is 70-100 ms post-SI response (Disbrow et al., 2001; Hari et al., 1984). It has been suggested that SII is involved in sensorimotor integration (Huttunen et al., 1996), haptic size and shape perception (Hsiao, 2008), guiding limb movement (Burton et al., 2002), integrating somatosensory information from both sides of the body (Manzoni et al., 1986; Ridley and Ettlinger, 1976), object manipulation, and tactile learning (Binkofski et al., 1999).

Electrophysiological recordings indicate that SI has feedforward connections to SII of both hemispheres, whereas SII has ipsilateral feedback connections to SI and contralateral callosal connections with SI and SII (Felleman and Van Essen, 1991; Qi et al., 2002). SII receives ipsilateral inputs from areas 3b and 1 that process cutaneous information, and area 3a which processes proprioceptive inputs (Qi et al., 2002). Additionally, some divisions of the

thalamus that receive afferent inputs from both cutaneous and deep receptors project to SII (Disbrow et al., 2002). Non-human primates and humans have secondary somatosensory (S2) and parietal ventral (PV) areas within SII. Neurons in S2 and PV have large receptive fields that combine cutaneous and proprioceptive inputs to determine the size and shape of objects (Disbrow et al., 2001; Fitzgerald et al., 2006a; Fitzgerald et al., 2006b). A mediolateral somatotopy exists within the lateral sulcus in the form of mirror-symmetric representations of the body surface within S2 and PV that are joined at the representations of the face (lateral), hands (intermediate), and feet (medial). More proximal parts of the body, for example, shoulder, trunk, and legs are represented further apart from this border in the anterior part of PV and the posterior aspect of S2 (Burton et al., 1995; Eickhoff et al., 2007; Qi et al., 2002).

Our previous MEG study (Popescu et al., 2012) using cutaneous stimulation of the hand have shown that the evoked neuromagnetic activity in SII is not consistently detected across subjects as the SI activity and, when present, it is highly variable in latency across subjects.

POSTERIOR PARIETAL CORTEX (PPC)

PPC is a somatosensory association area that consists of BA's 5 and 7, and is located in the postcentral sulcus, medial and posterior to the SI cortex hand area. PPC has dense interconnections with areas 1 and 2 of both ipsilateral and contralateral SI, and the thalamic association nuclei. Although PPC responds to some simple sensory stimuli, it is generally considered a hierarchically higher-level sensory processor than SI. Area 5 integrates complex tactile and proprioceptive information (Arezzo et al., 1981; Mountcastle et al., 1975), whereas area 7 integrates somatosensory and visual information (Hyvarinen, 1982; Sack, 2009).

Innocuous tactile stimulation activates the contralateral SI and PPC, and bilateral SII (Forss et al., 1994). Although PPC activation is historically linked to movement (Friston et al., 1997; Grafton et al., 1992), the contralateral PPC is activated by passive vibrotactile stimuli (Bardouille and Ross, 2008). Repetitive pneumotactile stimulation of the glabrous surface of the index and middle fingers using TAC-Cells modulates SI and PPC activity as a function of stimulus frequency (Popescu et al., 2012). SI and PPC adaptation profiles were quantitatively characterized, and the sensitivity to stimulation increases from SI to PPC. SII and PPC have more complex receptive fields and physiological properties when compared to SI. Very little is known about the response of these higher-order associative regions to repetitive stimulation of the face.

To achieve the objectives of Aim 1, we conducted MEG experiments using tactile stimulation of the right side of the face (at the nonglabrous oral angle), and the hand (at the glabrous surface of the distal phalanx of the right index finger) at 2 different frequencies (2Hz, 4Hz) with a newer, smaller TAC-Cell (Figure 1). Due to strong suppression of the SI response to consecutive pulses at 8 Hz (Popescu et al. 2010, 2012), we limited the face and hand stimulation to 2 and 4 Hz. The scaled-down version of the non-ferrous TAC-Cell displaces the skin directly via controlled pneumatic pulses and allows us to apply the stimulus within a confined area (e.g. a single digit). The main purpose of the new experiment is to compare the peak response adaptation of SI, SII, and PPC to repetitive unilateral stimulation of the hand and face as a function of stimulus frequency. We hypothesize that neuromagnetic responses generated in higher-order areas (SII and PPC) have a higher adaptation rate when compared to SI and adaptation will be a function of stimulus frequency. We also hypothesize that the peak

response latencies of SI, SII, and PPC will reflect the serial processing in areas of the cortical somatosensory network.

MECHANORECEPTORS

Mechanoreceptors are specialized sensory transducers that preferentially respond to mechanical strains that occur in the skin during function. Four types of mechanoreceptors have been distinguished by the following properties: 1) discharge rate to a sustained suprathreshold stimulus, and 2) receptive field and border size. Fast adapting (FA) receptors dynamically adapt to skin deformation, i.e. onset and sometimes removal of a stimulus. In addition to being dynamically sensitive, Slow-Adapting (SA) receptors signal the strength of a sustained stimulus that causes skin deformation. FA and SA receptors are further divided into Type I and Type II receptors. Type I receptors have small receptive fields with well-defined borders, whereas Type II receptors have larger receptive fields and less well-defined borders. The four different types of mechanoreceptors terminate in morphologically-different end organs: SA I – Merkel disks, FA I – Meissner's corpuscles, SA II – Ruffini endings, and FA II – Pacinian corpuscles. Merkel disks and Meissner corpuscles are present close to the skin surface, whereas Pacinian corpuscles and Ruffini endings are present in subcutaneous regions (Trulsson and Essick, 1997).

Each mechanoreceptor type has a distinct sensory function. Merkel disks have high spatial acuity (Johnson et al., 2000), and encode form and texture information because of their highly sensitivity to edges, points, and curvature. Meissner's corpuscles have low spatial resolution and are responsible for detection and discrimination of low frequency vibration. Pacinian corpuscles have a very low threshold to high frequency vibratory stimuli. Ruffini endings have been studied less extensively when compared to the other afferent types. Ruffini

endings are extremely sensitive to skin stretch and may be responsible for perception of the direction of the stimulus motion or the force that stretches the skin (Olausson et al., 2000).

On the basis of psychophysical and physiological experiments, it has been proposed that four distinct information processing channels mediate the human sense of touch in glabrous skin: one Pacinian (P) channel, and three non-Pacinian (NP I, NP II, and NP III) channels (Bolanowski et al., 1988). The P-channel mediated by the Pacinian corpuscles yields the sensation of vibration in the frequency range of 40 to 500 Hz. The NP I-channel mediated by the Meissner's corpuscles and RA fibers produces a sense of flutter in the 2 to 40 Hz range. The NP II-channel mediated by the Ruffini end organs and SA II fibers produces a "buzz" like sensation in the 100 to 500 Hz range. The NP III-channel mediated by the Merkel's disks and SA I fibers produces a sensation of "pressure" in the 0.4 to 2 Hz range. Sense of touch is mediated in hairy skin by the P, NP I, and NP II channels (Bolanowski et al., 1994).

DIFFERENCES BETWEEN OROFACIAL AND HAND ANATOMY

Execution of rapid and accurate hand movements (Flanagan et al., 2006; Wolpert and Ghahramani, 2000) during tasks involving fingers like pinch and grasp (Edin and Abbs, 1991) require continuous sensory afferent feedback from the cutaneous mechanoreceptors. Similarly, orofacial mechanoreceptors respond vigorously during natural movements like contact between the lips, air pressure generated during speech sounds, and facial tissue and mucosal deformation associated with voluntary lip and jaw movements (Johansson et al., 1988a). Orofacial muscles involved in the motor control of speech, suck, lick and swallow are distinct in morphology and structure when compared to most limb muscles (Chu et al., 2010). Histochemical and morphological analyses revealed an apparent lack of muscle spindle receptors and Golgi tendon organs (Connor and Abbs, 1998; Stal et al., 1987; Stal et al., 1990). Facial muscle fibers insert

directly into the skin rather than the connective tissue (Kennedy and Abbs, 1979) making them more susceptible to encode information about changes to muscle length and force rather than proprioceptive information. Pseudo-Ruffini endings (Nordin and Hagbarth, 1989) may serve some of the functionality to encode facial proprioception (Barlow, 1987; Barlow, 1998). Some jaw closing and tongue muscles have muscle spindles but differ in their morphology and composition when compared to limb muscles. Mechanoreceptors present in the human face also differ in type and distribution when compared to those present in the hand. SA units with high dynamic sensitivity and irregular discharge during sustained tissue deformation resemble the SA I units in the hairy and glabrous skin of the human hand (Johansson et al., 1988b). The SA afferent group with a regular discharge rate and spontaneous activity were similar to the SA II units in the human hand that are highly sensitive to lateral stretch. FA units are very common in both the hairy and glabrous skin of the hand but are less prevalent in the face. Properties of the few FA units that were observed in the face were similar to the FA I units found in the hand (Johansson et al., 1988b). But the classic Pacinian response present in the glabrous hand for vibratory input at 250 Hz is absent in hairy and glabrous perioral areas (Barlow, 1987; Johansson et al., 1988b; Nordin and Hagbarth, 1989).

AGE-RELATED CHANGES IN MECHANORECEPTORS

Healthy aging is accompanied by changes in sense of touch due to a decrease in sensory nerve function and a change in the size, number, and shape of afferent mechanoreceptors. Early use of cytological and nerve-staining methods (Cauna and Mannan, 1958) in the deep part of the human palmar corium, palmar subcutaneous tissue, at the sides of the middle and proximal phalanges adjacent to the periosteum determined that the size, and number of Pacinian corpuscles decreases with age. There is a significant correlation between the concentration of

Meissner's corpuscles (Bruce, 1980; Iwasaki et al., 2003) present in the distal phalanges and age. Histological and sensory tests reveal that older adults not only have a lower density of Meissner's corpuscles in the index finger, but their touch thresholds are 2 ½ times than those of younger subjects (Bruce, 1980). Vibration-threshold sensitivity of the pathways including the P-channel increases with age (Verrillo, 1979). Healthy older-adults require significantly higher amplitudes of vibration to achieve the same perception magnitude as younger subjects (Verrillo et al., 2002). Older-adults experience a loss of skin sensitivity in the thenar eminence at frequencies (40-600Hz) that primarily activate the P-channel (Verrillo, 1979; Verrillo, 1980). There is no significant loss of sensitivity at 25Hz, at which the response is mediated by NP channels. Changes in the size and shape of Meissner corpuscles and Merkel nerve endings have little effect on the threshold sensitivity and the low-frequency response of these receptors (Verrillo, 1979).

The loss of threshold sensitivity may be due to the decrease in the number of Pacinian corpuscles (Cauna, 1965). The progressive loss in sensitivity of the P-channels in older adults can be due to the fact that their sensitivity depends on the number of activated receptors (Gescheider et al., 2004). Less significant effects of aging are expected for the NP-channels as their sensitivities are nearly independent of the number of activated receptors (Gescheider et al., 2004). Lower skin temperatures can decrease the sensitivity of P-channels but not the NP systems. Decreased skin and core body temperatures in older adults (age > 65 years) may result in lower Pacinian corpuscle sensitivity (Verrillo, 1993).

Better knowledge of age-related changes in mechanoreceptor function could be crucial for the determining the prognosis or designing treatments for speech disorders following stroke or other neurological diseases that are common in older-adults (Wohlert and Smith, 1998). To

date, no quantitative information is available on the change in vibrotactile threshold sensitivity of the face as a function of age. Vibrotactile threshold detection of the face has been performed only in young adults (age-range = 20 to 30 years) (Andreatta and Davidow, 2006; Barlow, 1987; James et al., 2000). Facial skin is more compliant than skin on the finger-tip (Essick, 1998), and skin sensitivity is greater in females when compared to males (Essick et al., 1988). In Aim 2, we address this issue by determining the vibrotactile thresholds (at 5, 10, 50, 150, 250, and 300 Hz) at 2 sites on the face (right lower lip vermilion, and right nonglabrous surface of oral angle), and one site on the hand (index-finger) in group of healthy adults (younger adults: ages 18 to 30 years, older adults: ages 58 to 70 years). We hypothesize that the vibrotactile sensitivity thresholds will vary as a function of skin site, sex, and age of the participant.

In Aim 3, a novel-method is devised to measure the characteristics of the skin response to TAC-Cell stimulation. Differences in skin compliance and thickness between males and females may result in varying-degrees of skin displacement to the same stimulus amplitude. There is no existing device that demonstrates the method for real-time measurement of stimulus dependent tissue deformation, or quantification data of the resulting skin response. Reflectance dependent fiber-optic displacement sensors are used in industrial applications to measure the distance from an object that is moving parallel to the axis of the fiber-optic tip. A unique design (Aim 3) enables the use of these displacement sensors in concordance with the TAC-Cell (Figure 10). Skin response for different stimulus amplitudes were characterized as a function of the participants' sex. These responses were analyzed to measure the stimulus pressure, rise-fall times, mechanical response time, and the power spectrum for the different input amplitudes.

CHAPTER TWO: METHODS

PARTICIPANTS

Participants for the proposed studies (for all Specific Aims) were recruited via posted flyers and emails at the University of Kansas-Lawrence (KU-L), and through the NIH P30 Center for Biobehavioral Neuroscience Communication Disorders, Participant Research Core (PARC) at KU-L.

POWER ANALYSIS

A priori power analysis was conducted using Optimal Design 2.0 (Spybrook et al., 2008).

Aim 1

The sample size (n=9) selected for this study will yield statistical power greater than 0.80, medium-large effects size, and $p<.05$.

Aim 2

Results indicated that the sample size of 36 participants (level-2) provides 80% power to detect a relatively small effect (Glass's $\delta = 0.25$) even without subject- and trial-level covariates, under an expected effect size variance of .10. This sample size is also expected to achieve power of 1 when the effect size is in the medium to large range (i.e., $\delta = 0.37$). In sum, it is expected that the proposed study will be adequately powered with a sample of 36 participants (9 participants/group (younger females, younger males, older females, older males)).

Aim 3

The sample size (n=18) selected for this study is expected to provide statistical power greater than 0.80 to detect a relatively small effect (Glass's δ = 0.25). This sample size is also expected to achieve power of 1 when the effect size is in the medium to large range (i.e., δ = 0.37). This study is expected to be adequately powered with a sample of 18 participants (9 participants/group (younger females, younger males)).

INCLUSION CRITERIA

Aim 1: 9 healthy females (ages 18 to 30 years, Mean age = 24.2 years [SD=3.2])

Aim 2: 18 healthy younger adults (9 male, 9 female, ages 18 to 30 years), 18 healthy older adults (9 male, 9 female, ages 58 to 70 years)

Aim 3: 18 healthy younger adults (9 male, 9 female, ages 18 to 30 years)

Table 1: Participants information for Aims 2 & 3

Group	N	Age Mean ± SD
Younger Females	9	23.11 ± 1.93
Younger Males	9	24.44 ± 2.27
Older Females	9	63.67 ± 3.11
Older Males	9	64.78 ± 3.13

Participants were recruited for this study without exclusion based on race, or ethnicity. All participants were right handed according to the Edinburgh handedness scale (Oldfield, 1971) with no report of neurological or psychiatric illness, and not taking regular medication. For Aim 1, full written consent (approved by the KU Medical Center Institutional Review Board) and an

MRI safety screening form was obtained from all participants prior to study. For Aims 2 & 3, a full written consent approved by the KU-Lawrence Institutional Review Board was used.

EXCLUSION CRITERIA

Presence of neurological, sensory, or muscular deficits, metal implants such as (but not limited to): prosthetics, pacemakers, or vascular clips. Individuals, who are claustrophobic, have psychiatric abnormalities, or who are pregnant, with abnormal skin sensitivity on face or hand were excluded from the proposed study. Potential participants who are overweight (> 300 lbs) were excluded due to limitation of the maximum weight for the MEG system chair.

SPECIFIC AIM #1

TAC-CELL

The newer TAC-Cell (Figure 1) was custom molded (O.D. = 15mm, I.D. = 6mm, H = 6mm) with a 10/32" barb-fitting at the posterior surface of the stimulator. A custom non-commutated servo motor (H2W Technologies, Inc., Serial number: I 1101) coupled to a custom Airpel® *Anti-Stiction*® glass cylinder (Airpot Corporation) operating under position feedback (Biocommunication Electronics, LLC, model 511 servo controller) and computer control (Figure 2) was used to modulate the internal pressure of the TAC-Cell with pneumatic pressure pulses. The computer was equipped with a 16-bit multifunction card (PCI-6052E, National Instruments). Stimulus control signals were programmed with LabVIEW® software (National Instruments, v11.0) in our laboratory. These signals served as input to the servo controller, and were also used to synchronously trigger neuromagnetic data acquisition by the MEG scanner.

This hardware configuration achieves synchronization between stimulus generation and MEG data acquisition. A 15-foot thick wall polyurethane line (1/4" OD, 7/64″ ID) was used to

conduct the pneumatic stimulus pulse (10-90% intercept rise time = 8.5 ms) from the servo motor to the TAC-Cell placed on the participant in the MEG scanner. Mechanical response time (MRT), defined as the delay between leading edge of the pulse train voltage waveform and the corresponding TAC-stimulus displacement onset, was constant at 6 ms (Figure 3) for all stimulus rates. The reported peak dipole strength latency values were corrected for the MRT of the TAC-Cell.

Figure 1: TAC-Cell

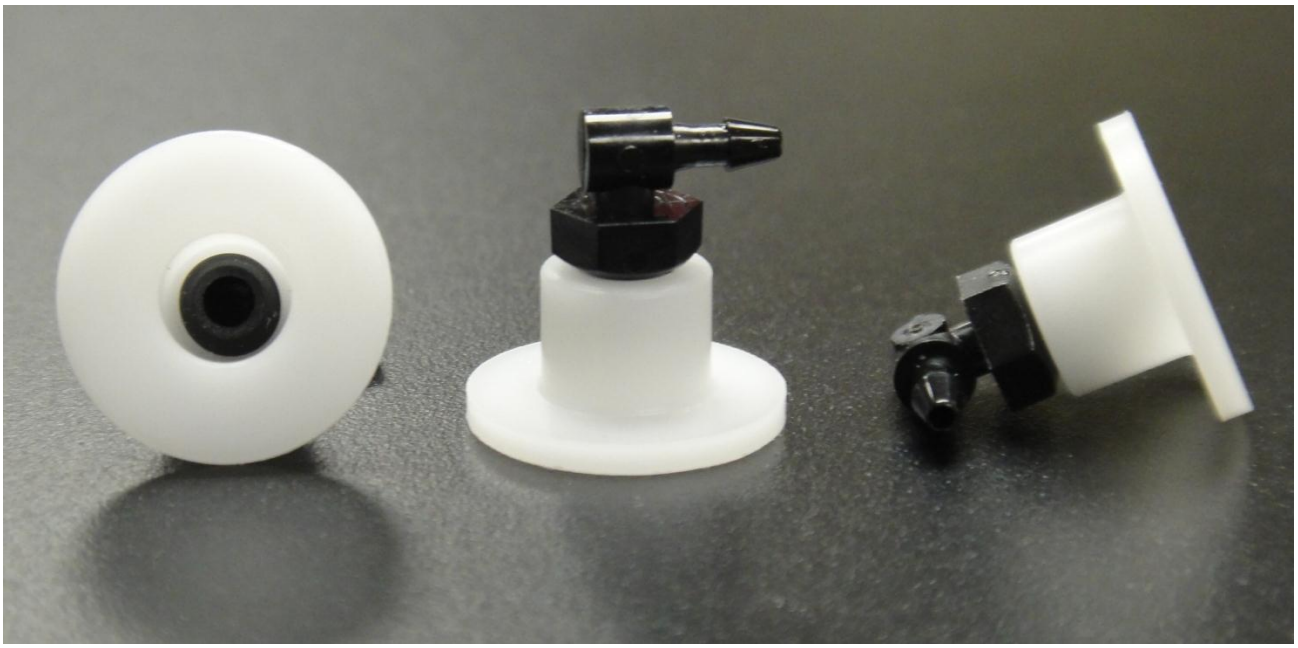

Figure 2: Schematic diagram for the TAC-Cell stimulus control system

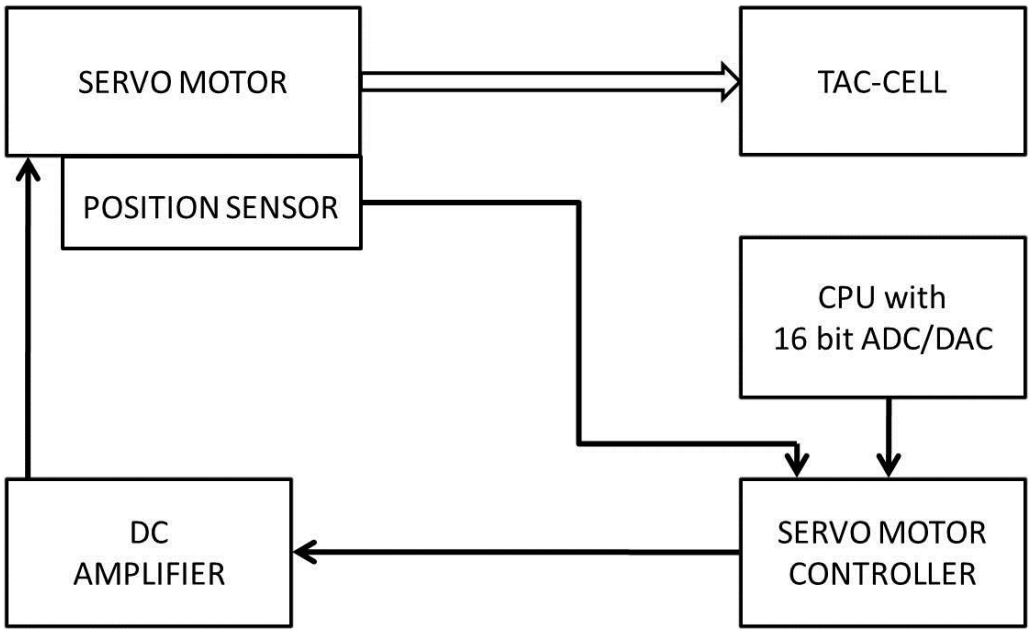

Figure 3: Mechanical Response Time (MRT) calculation

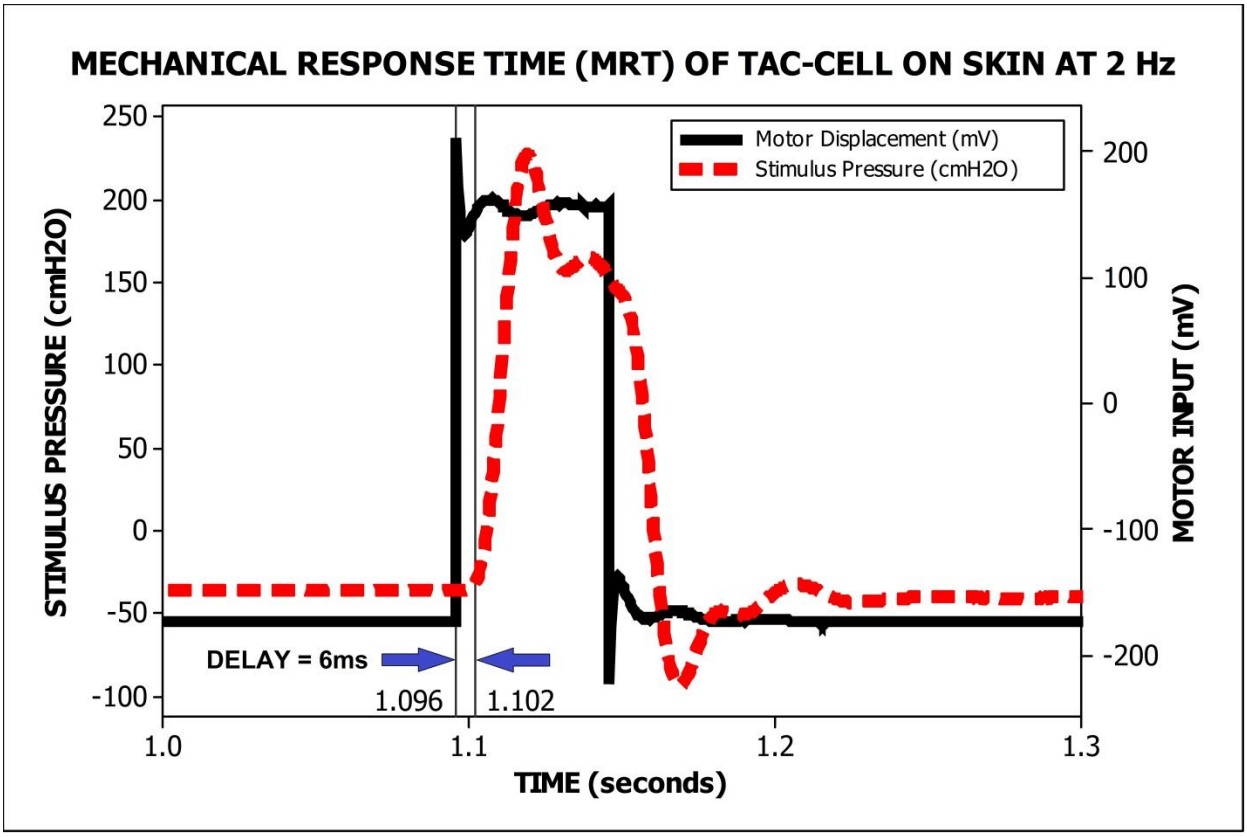

PARTICIPANT PREPARATION

A whole-head MEG system (CTF Omega) equipped with 151 axial-gradiometer sensors was used to record the cortical response to the TAC-Cell inputs. Prior to the MEG recording session, each participant was instrumented with:

- Three localization coils were placed at nasion, left and right preauricular points, respectively, to determine the head position with respect to the sensor array.
- Two bipolar EEG channels were used to record electrooculograms (EOG) in order to identify trials affected by ocular movement artifacts and eye-blinks.
- TAC-Cell on the face at the nonglabrous surface of right oral angle or the hand at the glabrous surface of the right index finger using double adhesive collars (Figure 4). Velcro fasteners were used to secure the TAC-Cell. Stimulus site and frequency was counterbalanced among participants.
- Following the MEG recording session, registration landmarks were placed at the same three positions of the localizing coils. TAC-Cells were removed from the skin sites, and participants were immediately placed inside a MRI scanner in an adjacent suite to image their brain anatomy.

STIMULUS PARADIGM

Pneumatic servo control was used to produce pulse trains [intertrain interval of 5 s, 125 reps/train rate] (Figure 5). Each pulse train consists of 6-monophasic pulses [50-ms pulse width]. Short-term adaptation of the cortical neuromagnetic response to TAC-Cell patterned input was assessed

using a randomized block design of two pulse train rates, including 2 and 4 Hz at each skin site. The 2 and 4 Hz stimulus blocks lasts for approximately 16 and 14 min respectively.

Figure 4: Participant Preparation

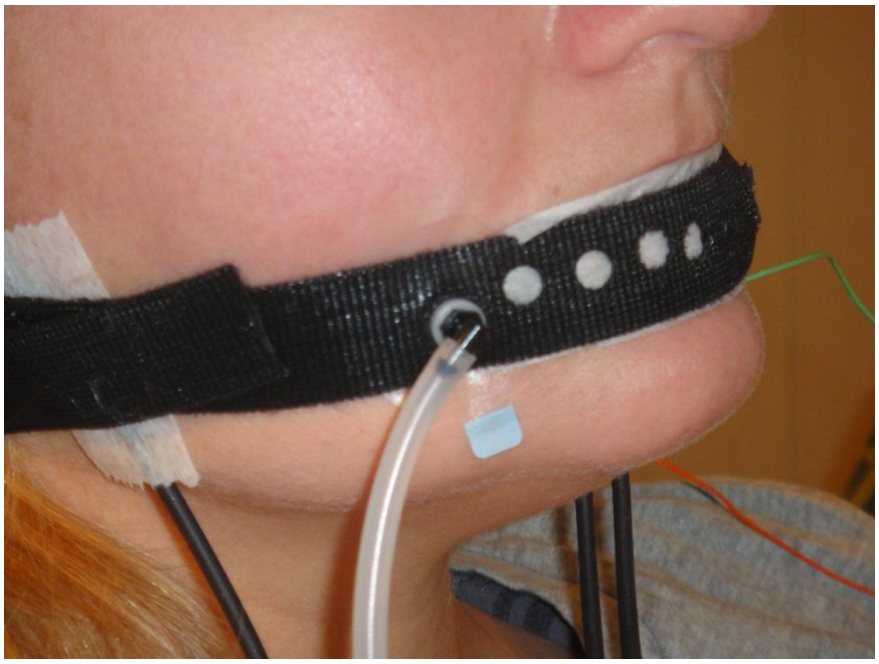

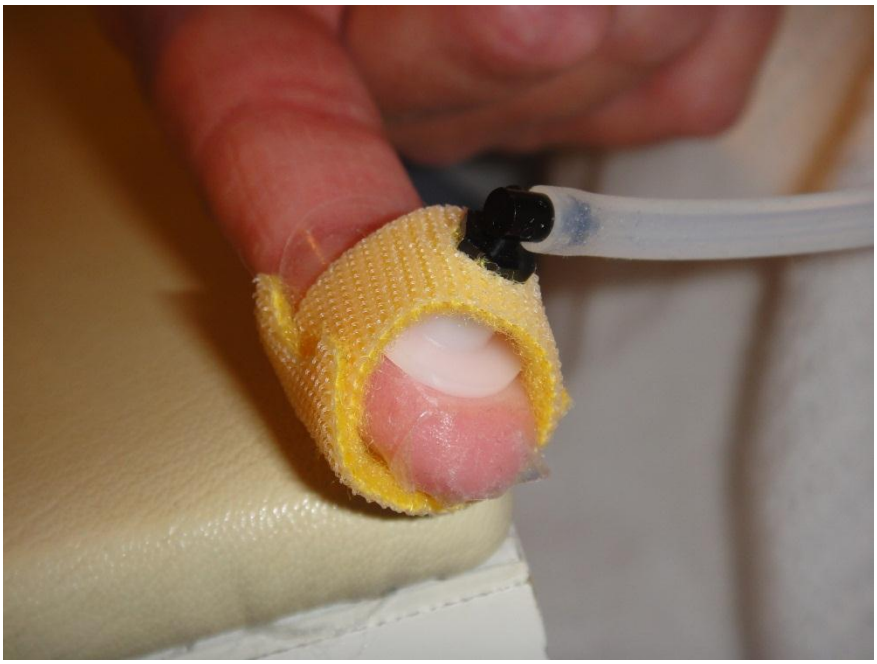

Figure 5: Stimulus Paradigm

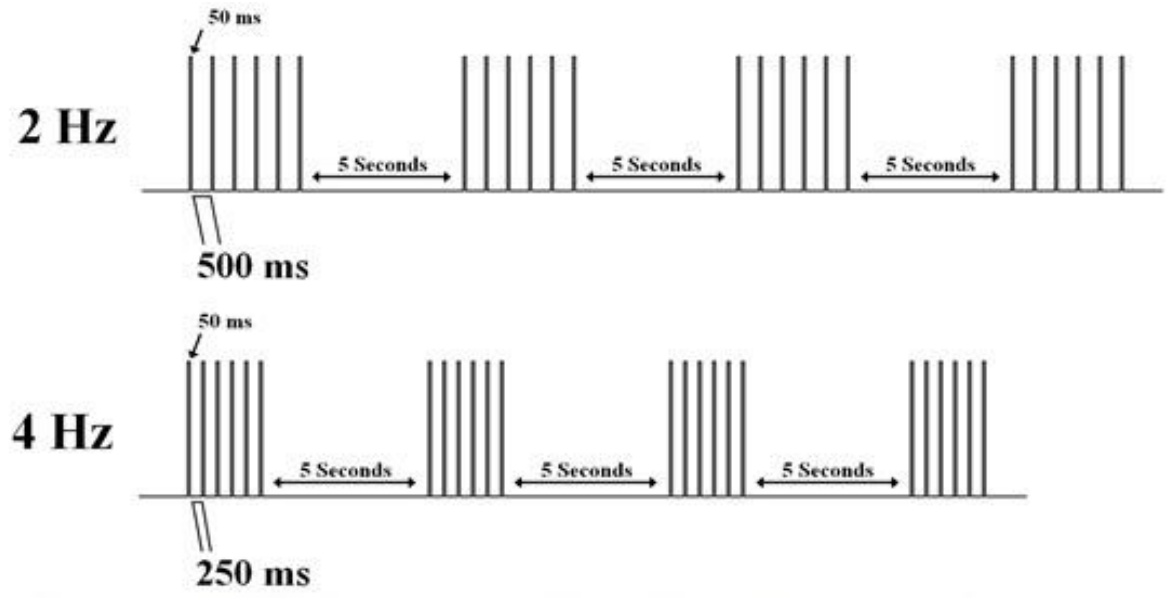

MEG DATA ANALYSIS

DATA PRE-PROCESSING

The MEG data was digitally bandpass filtered between 1.5 Hz and 50 Hz using a bidirectional 4th order Butterworth filter. Trials corresponding to 1s before and after the stimulus were visually inspected for artifacts and those containing movement or eye-blink artifacts were discarded. The remaining trials for each experimental condition were averaged and the DC was offset using the pre-stimulus period as baseline. No less than 90 trials per participant in each experimental condition were used in averaging. For an accurate source estimation of the multiple component response, the averaged datasets for each participant and condition were decomposed using a PCA-filtering ICA algorithm (Delorme and Makeig, 2004). PCA-filtering was applied to reduce the data dimensionality, and to segregate the contribution of each independent component (IC) to the overall magnetic field.

SOURCE RECONSTRUCTION

For each dataset, the source reconstruction was performed separately for each IC in CURRY (Compumedics Neuroscan), using a spherically symmetric volume conductor model fitted to the skull (segmented from the MRI data). The source space was defined as a regular grid of points in the brain volume (average distance between points was 5 mm). Since the independence constraint in ICA relies entirely on the amplitude distribution of the sensor data and does not include assumptions about the underlying sources, each IC can reflect the activity of single or multiple synchronous neuronal generators (Delorme and Makeig, 2004; Hironaga and Ioannides, 2007; Vigario et al., 2000). Accordingly, the ICs of interest were localized using a two-step source reconstruction algorithm. First, a current density analysis using sLORETA (Pascual-Marqui, 2002) was performed to verify if single or multiple regional generators account for each IC and to identify the corresponding spatial peaks of activity. sLORETA uses the standardization of a minimum norm inverse solution, and does not require a priori information about the number of active sources. Second, a location constrained dipole analysis (with the positions of the dipoles at the spatial peaks of activity retrieved by sLORETA) was performed to obtain estimates of the direction and strength for each active brain region. The dipole fitting procedure allows characterizing the source strengths using current units rather than the statistical measures retrieved by sLORETA.

STATISTICAL ANALYSIS

An Analysis of Variance (ANOVA) was performed with peak dipole locations, strengths, and latencies as dependent variables. Stimulation site (hand, face), pulse index number (1, 2, 3, 4, 5, 6), stimulus frequency (2, 4 Hz), and response components (SI, PPC) were used as the

independent variables. This analysis allows us to examine how these variables, and their interactions influence the SI, SII, and PPC peak dipole strength adaptation **(Aim 1a),** and their response latencies **(Aim 1b)**. Statistical analysis for this study was performed using IBM SPSS Statistics software (*v. 20*)

HYPOTHESES

H_0 #1a (Aim 1a). For Aim 1a, it is hypothesized that there will be a significant difference between the peak dipole strength adaptation rates across different areas of the cortical somatosensory network. It is also hypothesized that the rate of adaptation will be significantly different between the 2 stimulus frequencies (2 Hz, 4 Hz), with the adaptation rate of the peak dipole strength at 4 Hz expected to be significantly higher than at 2 Hz for corresponding somatosensory areas in the hand and face stimulation conditions.

H_A #1a (Aim 1a). The alternate hypothesis suggests that SI, SII, and PPC peak dipole strength adaptation measures will not modulate as a result of TAC-Cell stimulation. Our earlier findings (Popescu et al., 2012) obtained when cutaneous stimulation was applied simultaneously at multiple digits indicated a significant difference between rates of adaptation of the SI vs. higher order cortical areas in response to TAC-Cell stimulation of the hand. If findings from stimulation of single digits are different, this can be reflective of a substantial effect of the integration of multiple cutaneous inputs on the adaptation rate.

H_0 #1b (Aim 1b). For Aim 1b, it is hypothesized that there will be a significant difference between the peak dipole strength latencies of SI, SII, and PPC for hand/face stimulation, which will provide support to a hierarchical processing in areas of the cortical somatosensory network. In addition, response peak latencies at both stimulation frequencies are

expected to be significantly lower for face stimulation when compared to hand stimulation because of the shorter conduction time of the trigeminal pathway.

H_A #1b (Aim 1b). The alternate hypothesis states that there will not be a significant difference between the SI, SII, and PPC peak dipole strength latencies or between face vs. hand stimulation. This would contradict studies that have indicated shorter neural response latencies for face stimulation when compared to hand stimulation (Popescu et al., 2012; Popescu et al., 2010; Venkatesan et al., 2010).

SPECIFIC AIM #2

VIBROTACTILE DETECTION THRESHOLD (VDT) ASSESSMENT FOR HAND AND FACE

An established psychophysical protocol was used to assess cutaneous vibrotactile sensitivity (Aim 2) in the lower face and hand (Andreatta and Barlow, 2003; Andreatta et al., 2003; Andreatta and Davidow, 2006; Andreatta and Barlow, 2009; Barlow, 1987). A National Instruments cRIO real time embedded controller is programmed to synthesize (NI 9263, 16-bit, 100KS/s) sinusoidal bursts that are ramped up to an on-state for 1 s, and ramped down to an off-state for 1 s. A linear rise-fall decay function of 100 ms circumvents mechanical transients. This signal is conditioned by a Bruel & Kjaer model 2706 power amplifier and input to a Bruel & Kjaer model 4810 Minishaker. The Minishaker includes custom fixtures and sensors (Figure 6) for precision vibrotactile stimulation and measurement, a stainless steel shaft and nylon contactor probe (Area=0.5 cm^2), a stainless steel rigid surround (annular gap at 1 mm) bolted to a linear translation stage with integral micrometer. This configuration allows the surface of the rigid surround to be adjusted relative to the contactor probe to produce a 1000 μm tissue preload

against the moving stimulator probe. A Schaevitz microminiature displacement sensor provides an output signal that is linearly related to contactor probe displacement from DC to 800 Hz (resolution 0.01 μm). Participants were seated in a dental examination chair with an articulating headrest, and were asked to press a response button when they detected the vibratory stimulus. A single-interval up/down (SIUD) adaptive procedure was used to estimate vibrotactile thresholds (Lecluyse and Meddis, 2009) for stimuli presented at 5, 10, 50, 150, 250, and 300 Hz at two sites on the face, including the right nonglabrous surface of the oral angle (Figure 8), and the right lower lip vermilion (Figure 9); and on the hand at the glabrous surface of the distal phalanx of the right dominant index finger (Figure 7). Test order for site and frequency was randomized among participants. Participants wore earphones with narrow-band noise centered at the 5, 10, 50, 150, 250, and 300 Hz test frequencies to mask the acoustics associated with the minishaker.

Figure 6: Bruel & Kjaer model 4810 Minishaker

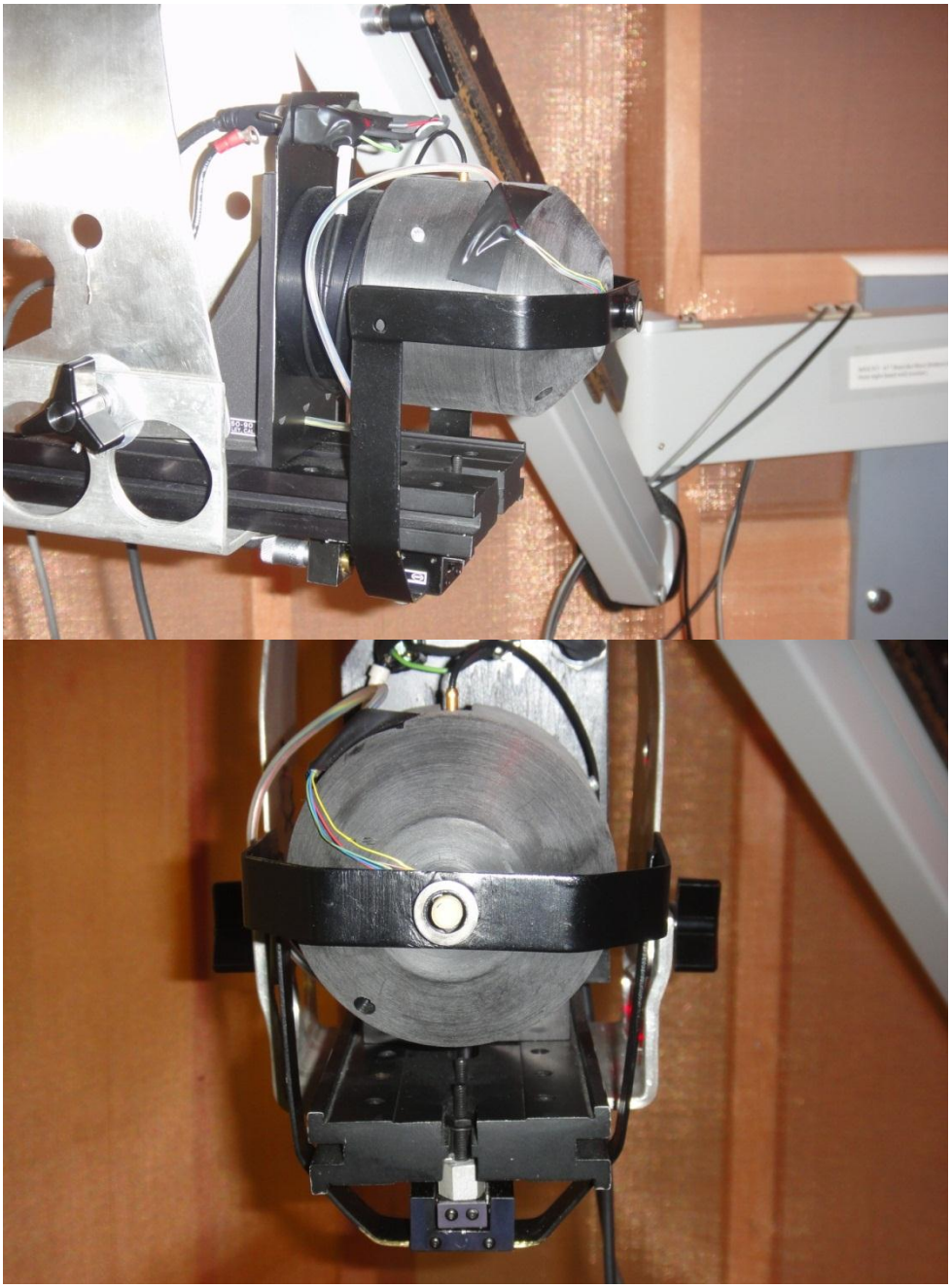

Figure 7: Positioning of the minishaker for index finger stimulation

Figure 8: Positioning of the minishaker for stimulation of non-glabrous surface of the oral angle

Figure 9: Positioning of the minishaker for stimulation of lower lip vermilion

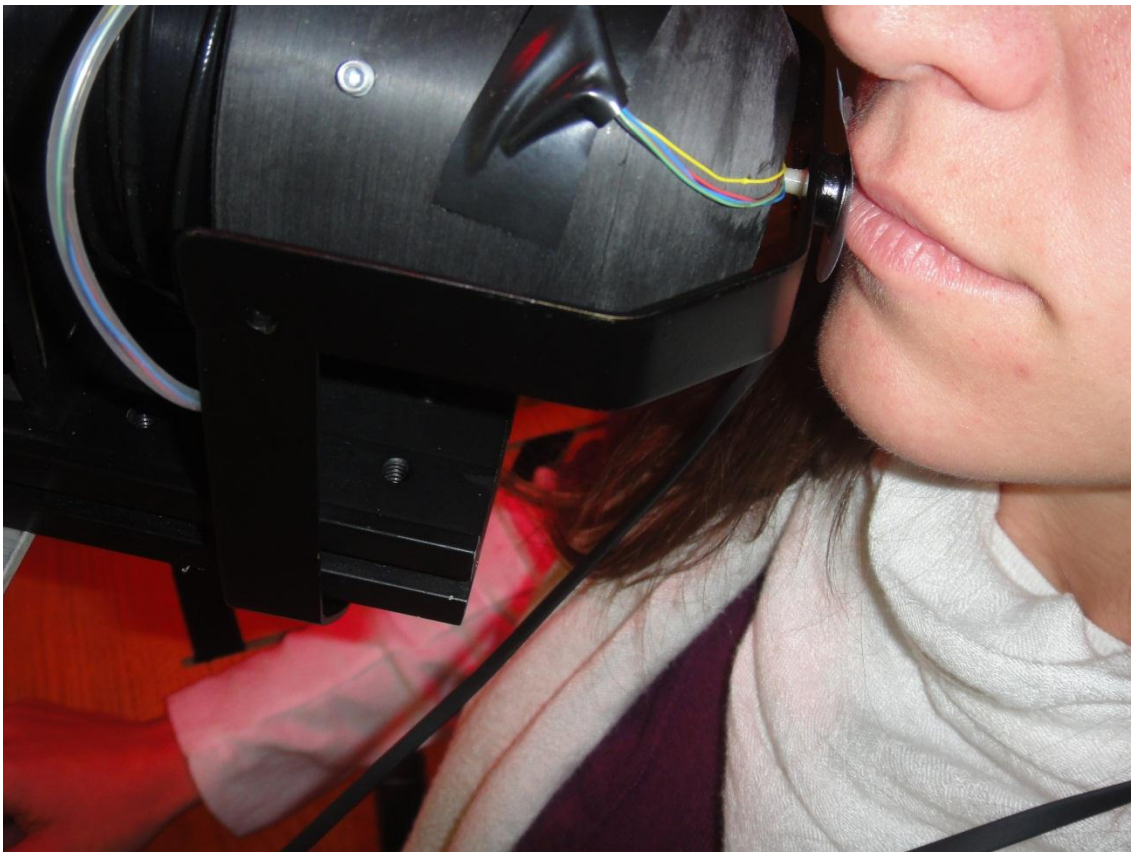

STATISTICAL ANALYSIS

ANOVA was used to estimate the effects of skin site (hand vs. cheek vs. lower lip), test frequency (5, 10, 50, 150, 250, and 300 Hz), participants' age (young vs. old), participants' sex (male vs. female) and their interactions on VDT's. This analysis will allow us to determine how age (**Aim 2a**), sex (**Aim 2a),** skin site (**Aim 2b**), and their interactions impact the VDTs.

HYPOTHESES

H_0 #2a (Aim 2a). For Aim 2a, it is hypothesized that there will be a significant difference between the vibrotactile sensitivity thresholds at the skin sites as a function of age, sex, and their interactions. Increase in age results in changes in density and morphology of mechanoreceptors. But changes in the number and morphology of Meissner's corpuscles and Merkel's disks do little to alter their vibration sensitivity. The sensitivity of the P-channels increase with age, and less significant effects of aging are expected for the stimulation sites on the face as they lack the Pacinian-type corpuscles. It is expected that the vibrotactile sensitivity thresholds will increase as a function of age for finger stimulation, but remain unaltered for face stimulation. It is also expected that vibrotactile sensitivity thresholds will depend on the participants' sex due to differences in tactile sensitivity between males and females.

H_A #2a (Aim 2a). The alternate hypothesis states that vibrotactile sensitivity thresholds will not vary as a function of age or sex. This would contradict many studies that indicate that vibrotactile sensitivity thresholds vary as a function of age (for finger stimulation) and sex (Gescheider et al., 2004; Verrillo, 1979; Verrillo, 1980; Verrillo et al., 2002).

H_0 #2b (Aim 2b). For Aim 2b, it is hypothesized that there will be a significant difference between the vibrotactile sensitivity thresholds as a function of skin site (hand, face). It is expected that the vibrotactile sensitivity thresholds will modulate as a function of skin site.

H_A #2b (Aim 2b). The alternate hypothesis states that vibrotactile sensitivity thresholds will remain the same regardless of skin site. This would contradict the studies which indicate that vibrotactile sensitivity thresholds modulate as a function of skin site (Barlow, 1987; Essick et al., 1988) due to the differences in orofacial and hand anatomy (see review).

SPECIFIC AIM #3

CHARACTERIZATION OF THE TAC-CELL STIMULUS

Subsequent to the VDT assessment, the effects of the pneumotactile pulses on skin displacement were examined (Aim 3) using a reflection dependent non-contact fiberoptic displacement sensor (Figure 10). A linear translation stage (Newport optics, Model M-423) was coupled to a heavy-duty base-mounted optical support rod (Newport optics, Model 45) (Figure 10). The TAC-Cell used for Aim 3 consists of a 3.25 mm PFA flange adhered to a custom-built 0.2-ml Ludwig-style vial with 6.5 mm ID (Savillex, vial part no. 200-902-60). The TAC-Cell was glued to a non-contact fiberoptic displacement sensor (PHILTEC, Model D170) at an end-gap distance (end-end distance between the active-surfaces of the TAC-Cell and the sensor) of 8mm (see Calibration, Figure 13). The sensor was mounted on the linear stage allowing for precise placement of the TAC-Cell on the subject. Stimulus pressure (calibrated in cmH_2O) was measured using a pressure transducer (Honeywell, 1 psi full scale) that was attached to the 15-foot fuel line (I.D. = 7/64") carrying the pneumatic stimulus from the motor to the active surface of the TAC-Cell. A stainless steel marker (diameter = ¼") was glued to the glabrous skin overlying the distal interphalangeal joint of the right index finger (Figure 11). The marker was aligned such that its placement is within the ID of the active surface of the TAC-Cell and is parallel to the axis of the sensor. The linear stage containing the TAC-Cell was lowered and the TAC-Cell attached to the finger using a double adhesive collar (Figure 11 and 12).

Stimulus amplitude was varied using different motor inputs (1V, 0.8V, 0.6V, 0.4V), and the corresponding skin displacement peaks were measured. The input stimulus consists of ten 50-ms pulses that were generated at 2 Hz. Peak values for skin displacement were averaged

over the 10 pulses for each input stimulus. LabChart Pro (*v 7.3*, ADInstruments) was utilized to sample (1k samples/s) the skin displacement signals from the fiberoptic sensor, pressure signals from the pressure transducer, and LVDT input to the servo motor (Figure 14). The Peak Analysis Module in LabChart was used for offline analysis of the peaks and 10-90% rise and fall times in the recorded data (displacement in mm, pressure in cmH_2O).

Figure 10: TAC-Cell attached to fiber-optic displacement sensor

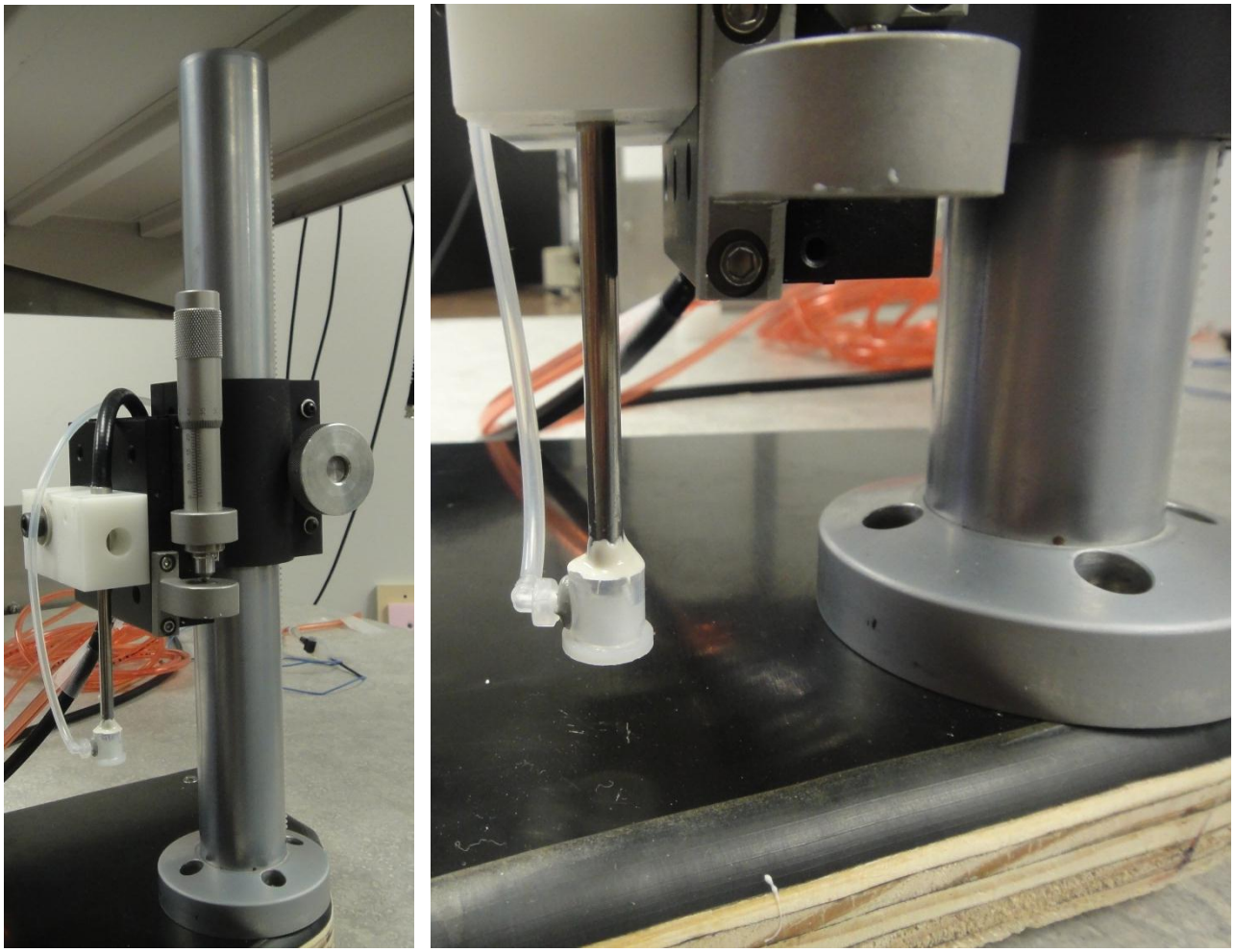

Figure 11: Placement of the stainless-steel marker and double-adhesive collar on the index finger

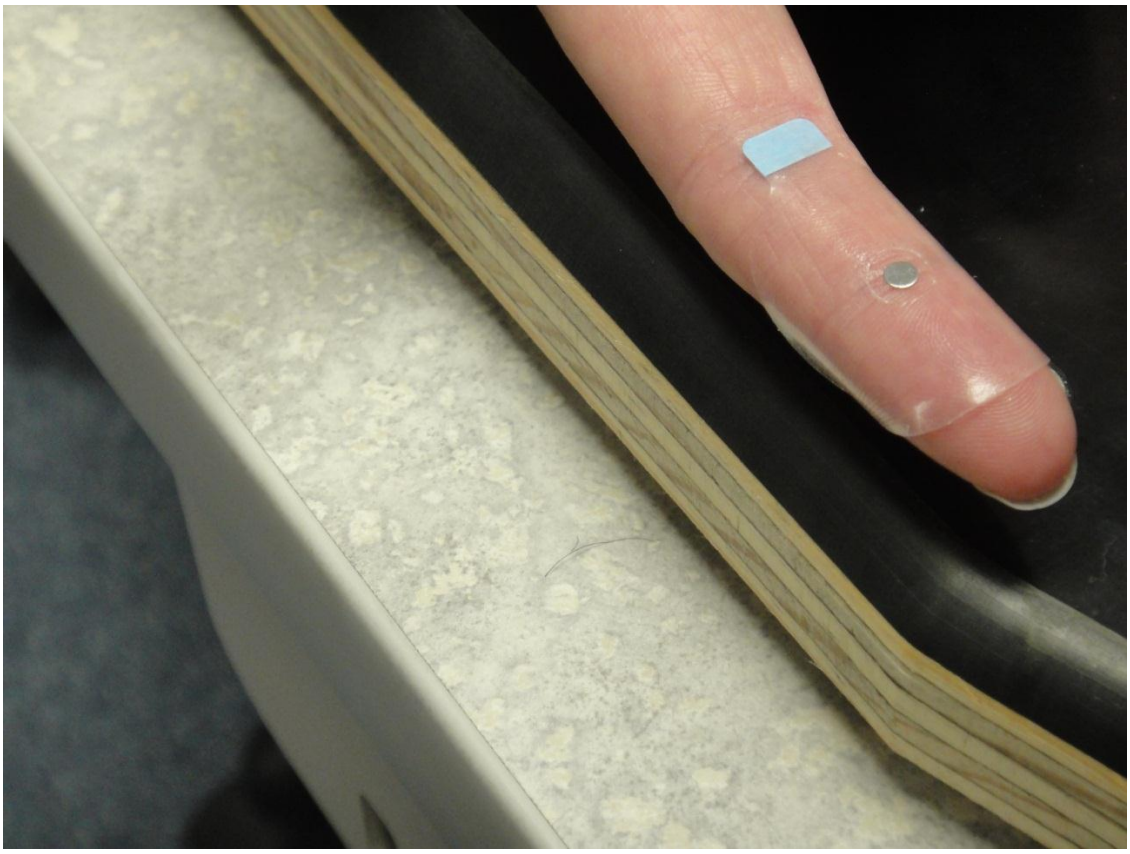

Figure 12: Placement of the TAC-Cell on the index finger

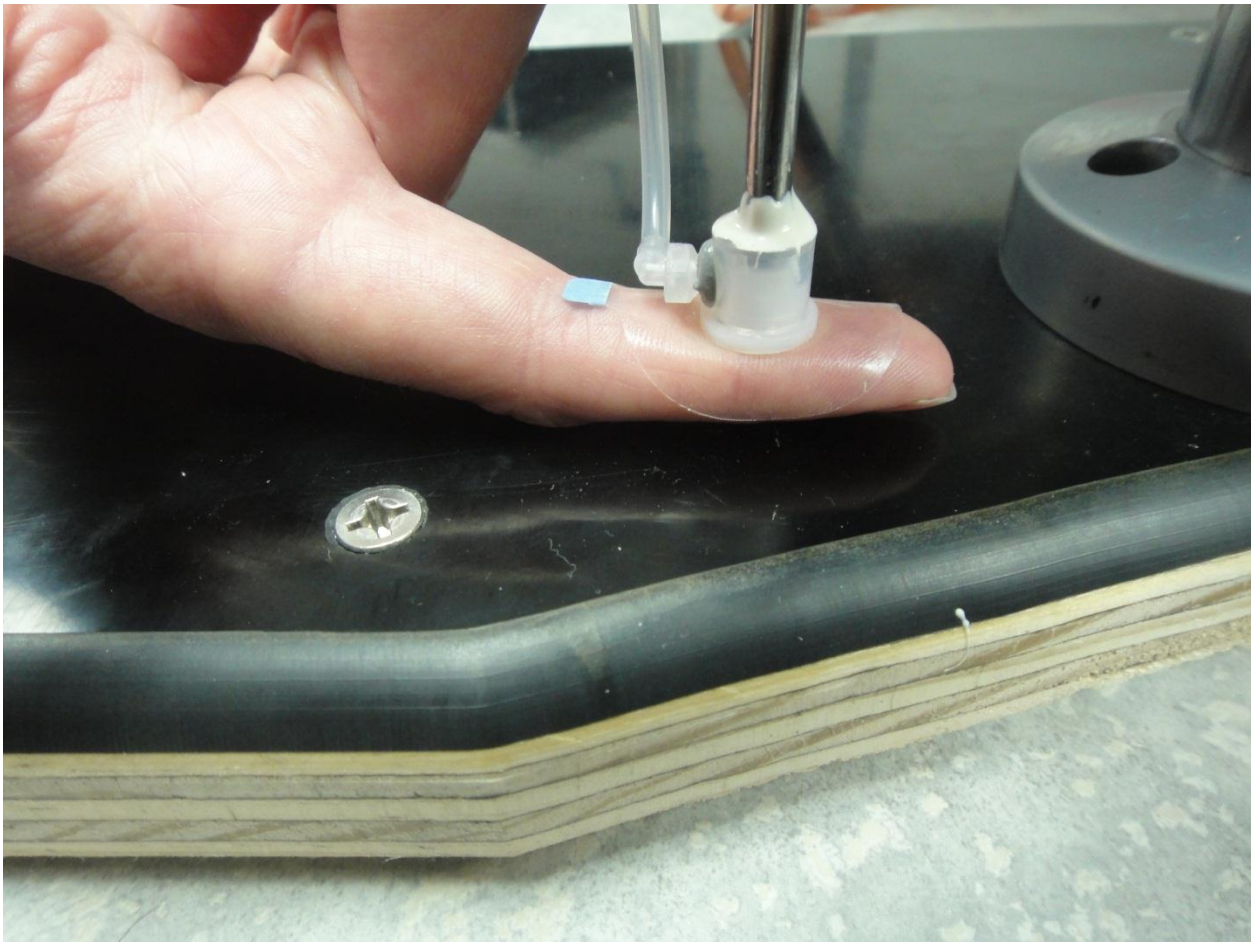

CALIBRATION

Distance between the stainless steel marker and the surface of the fiber optic sensor was varied in increments of 0.5 mm and the corresponding outputs from the sensor were recorded. It was determined that the linear-operating range of the sensor was between 2 and 13 mm (R^2 = 0.99) (Figure 13). The TAC-Cell was affixed at an end-gap distance of 8 mm, so that the range of motion of the stainless-steel marker is within the linear-operating range of the sensor. A linear regression model was used to fit these variables (sensor output, distance from the marker).

LabChart Pro's multi-point calibration was used to accurately scale the output variables based on the values obtained using the regression model (Figure 13).

Figure 13: Fiber-optic sensor calibration

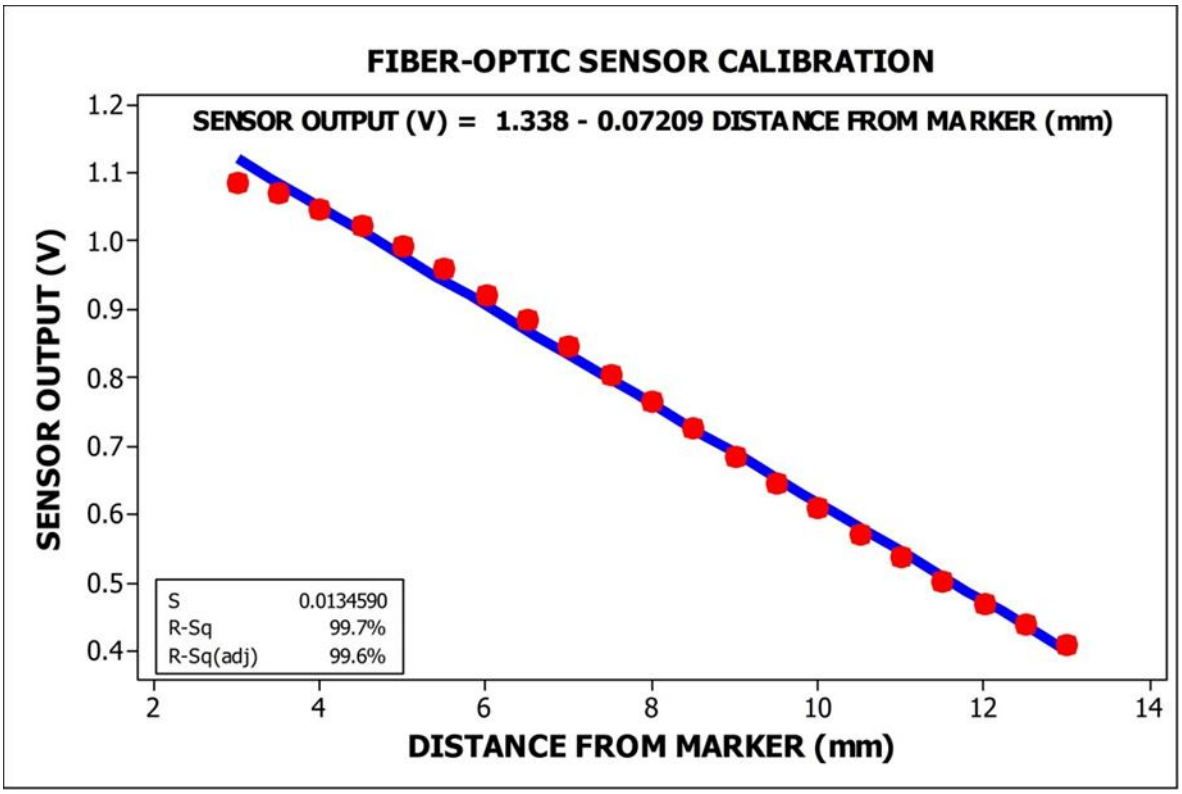

STATISTICAL ANALYSIS

ANOVA was used to estimate the effect of different stimulus input amplitudes (dependent variable) on skin displacement as a function of participants' sex, and their interactions.

HYPOTHESES

H_0 #3 (Aim 3). For Aim 3, it is hypothesized that skin displacement amplitudes depend on the participants' sex and varies as a function of the stimulus input amplitude (motor input).

H_A #3 (Aim 3). The alternate hypothesis suggests that skin displacement amplitudes may vary as a function of the stimulus input amplitudes but there is no significant difference based on participants'sex.

Figure 14: Example of skin displacement and stimulus pressure data for 6 input pulses at 2 Hz when motor input = 1V

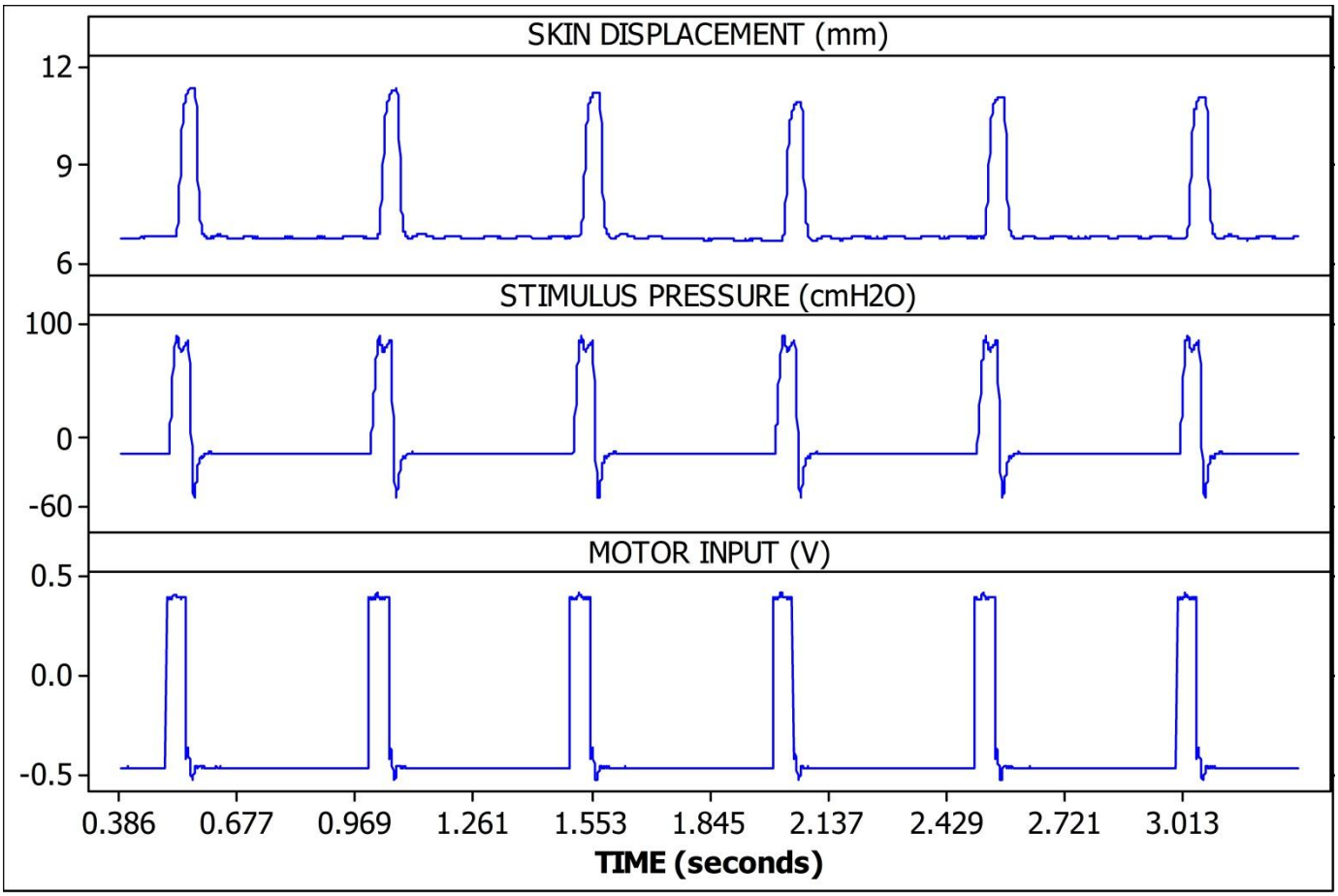

CHAPTER THREE: RESULTS

SPECIFIC AIM #1

NEUROMAGNETIC SEFs

An illustration of the averaged neuromagnetic responses' (overlay of all 151 MEG sensors) somatosensory evoked fields (SEFs) due to hand stimulation at 2 Hz is shown in Figure 15 for one participant. The first two components are characterized by dipolar magnetic field patterns confined to the contralateral (left) hemisphere; the third component is characterized by a bilateral magnetic field distribution (shown in left and right views). Each pulse stimulus in the train produced transient neuromagnetic responses with a timevarying morphology indicating the existence of multiple SEF sources that peak at different latencies. The first component of the response peaks in this example was at 68 ms, whereas the second component peaks was observed at 98 ms. Each of these two components is characterized by a unilateral, distinctly dipolar pattern of the magnetic field (Figure 15), confined to a different subarray of sensors in the left hemisphere (contralateral to the stimulation site). These two components are followed by a third component peaking at 125 ms, which is characterized by a bilateral dipolar pattern of the magnetic field that suggests bilateral activity evoked in SII areas, as shown by MEG studies using electrical stimulation paradigms (Forss et al., 1994; Hari et al., 1993). The dipolar pattern at the peak of the third component is asymmetric over the subarray of sensors covering each hemisphere (e.g., the negative magnetic field recorded by the posterior lateral sensors in the left hemisphere is higher than the positive magnetic field in left anterior lateral sensors). Subsequent pulses within the train evoke similar SEFs, although with different relative amplitudes of the components. Two observations regarding the inter-subject variability in the SEF responses at the

sensors are worth mentioning. First, visual inspection of the two leading response components evoked by the first pulse in the train (i.e., without considering the effect of their short adaptation patterns induced by the subsequent serial pulses) indicated that their relative amplitude was different between subjects, with the amplitude of the first component being higher compared to the second component in some subjects, and lower in others. In addition, it was observed that the first 2 prominent components were followed by a series of other late response components (including the bilateral third component described above), with a markedly high inter-subject variability in latency and magnetic field topography (i.e., the sequence and/or characteristics of these late response components were not consistent across subjects). Suppression and inconsistency of SII activity among subjects was also observed for face stimulation.

Figure 15: Illustration of the averaged neuromagnetic response due to hand stimulation at 2 Hz for one participant

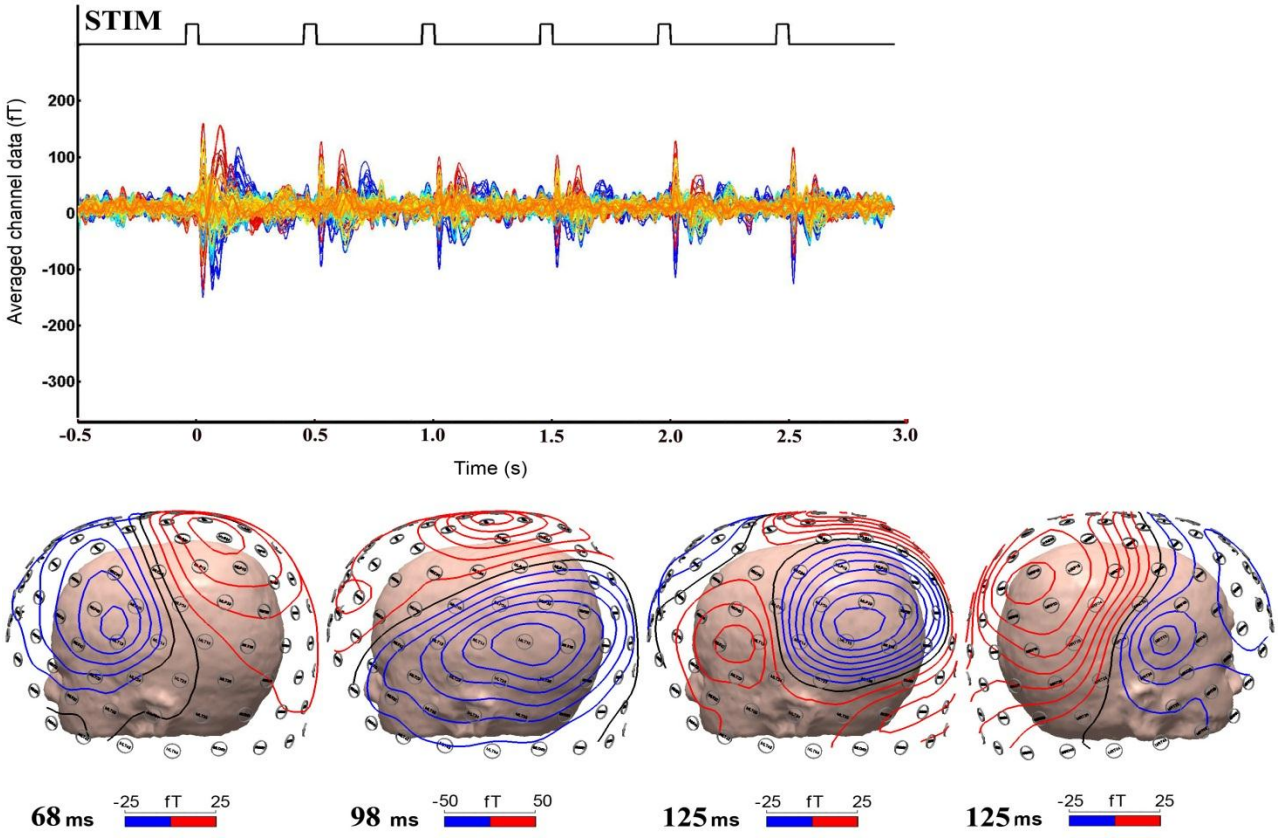

SOURCE LOCATIONS

Hand stimulation resulted in the activation of the contralateral SI, and PPC areas (Figures 16, 17, and 19), while face stimulation invoked a response in the contralateral SI cortex (Figures 17 and 18). The results of source estimation (i.e., current density reconstruction using sLORETA) are shown for each of the ICs that correspond to SI and PPC SEF response components for hand stimulation (Figure 16), and SI components for face stimulation (Figure 17). The activity maps shown on the cortical surface at the peak latency of the first pulse in the train (for 2 Hz stimulation frequency) are clipped at 80% of the spatial maximum for each source. Consistent with our previous studies where multiple digits or both lip vermilions were stimulated (Popescu et al., 2012; Venkatesan et al., 2010) , the SII response was variable in latency and inconsistent across subjects for both hand and face stimulation. In addition, the PPC activity could not be identified for face stimulation using conventional analysis. When present in the hand stimulation condition, the suppression of SII response was similar to the one observed in our earlier study (Popescu et al., 2012) that used the larger TAC-Cells. The results of source reconstruction (i.e., sLORETA-constrained dipole fitting) are exemplified in Figures 18 & 19 on T1-weighted MRI orthogonal images. For the early (first) response component, dipoles were localized in the anterior wall of the postcentral gyrus, consistent with generators in the proximal neuronal populations of SI areas 3b and 1. Dipoles for the second response component that was observed for hand stimulation was localized in regions of the post-central sulcus, posterior, and slightly medial with respect to the SI source. The results are in agreement with the somatotopic organization of the primary somatosensory cortex with the face SI source represented more towards the base of the postcentral gyrus, i.e. more laterally, anteriorly, and inferiorly than the hand SI. The PPC component for hand stimulation was more medial (mean Δx = 3 mm, SD = 5

mm), more posterior (Δy = -4 mm, SD = 10 mm), and more superior (Δz = 2 mm, SD = 3 mm), and the peak dipole location was consistent with our previous study (Popescu et al. 2012).

Figure 16: Results of current density reconstruction is shown for SI (a) and PPC (b) for the hand stimulation condition

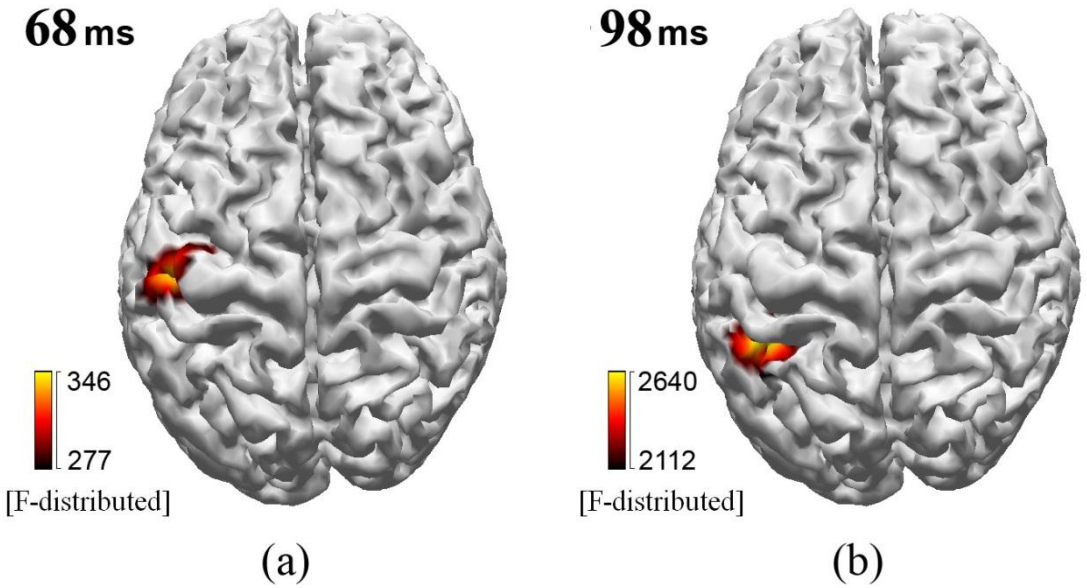

Figure 17: Results of current density analysis at the peak latency of the SI response for the hand (a) and face (b) stimulation conditions

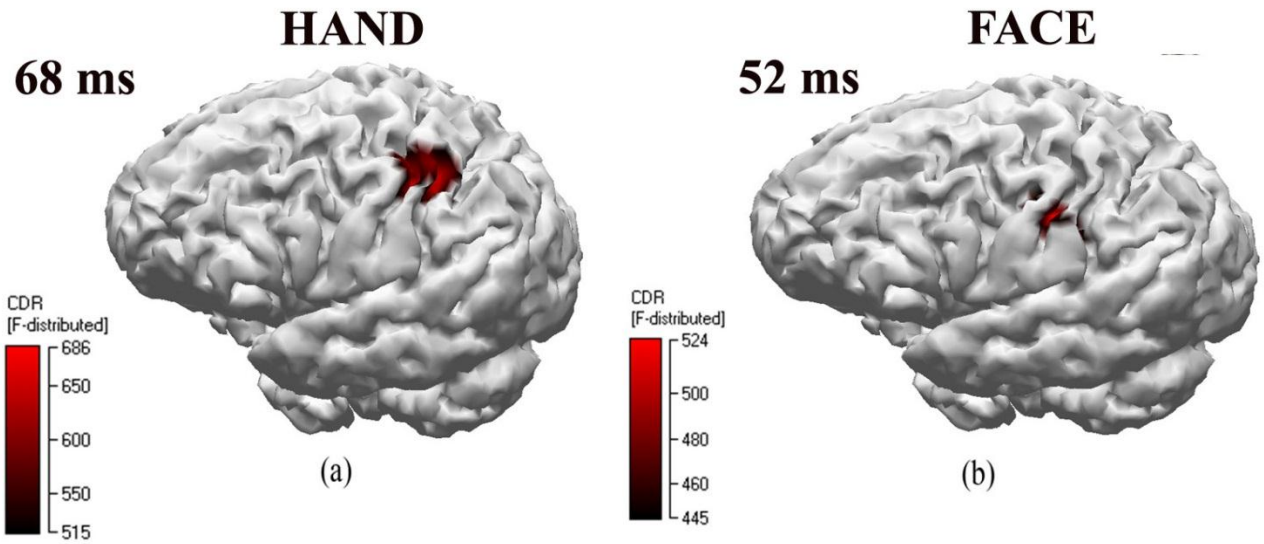

Figure 18: Dipole locations are shown in orthogonal axial and sagittal MRI slices for the SI during face stimulation.

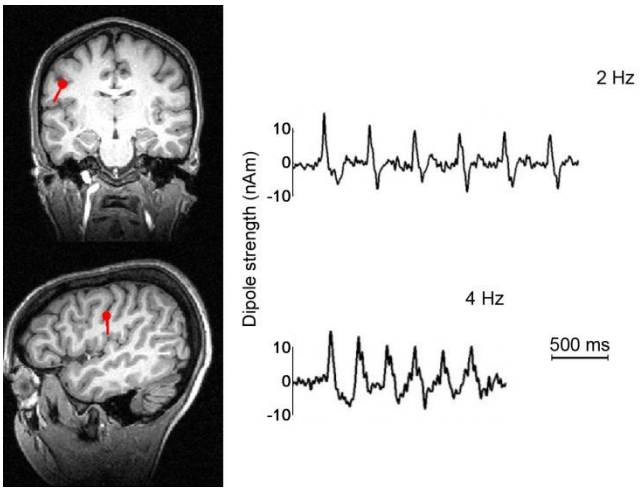

Figure 19: Dipole locations are shown in orthogonal axial and sagittal MRI slices for the SI (a) and PPC (b) activation during hand stimulation.

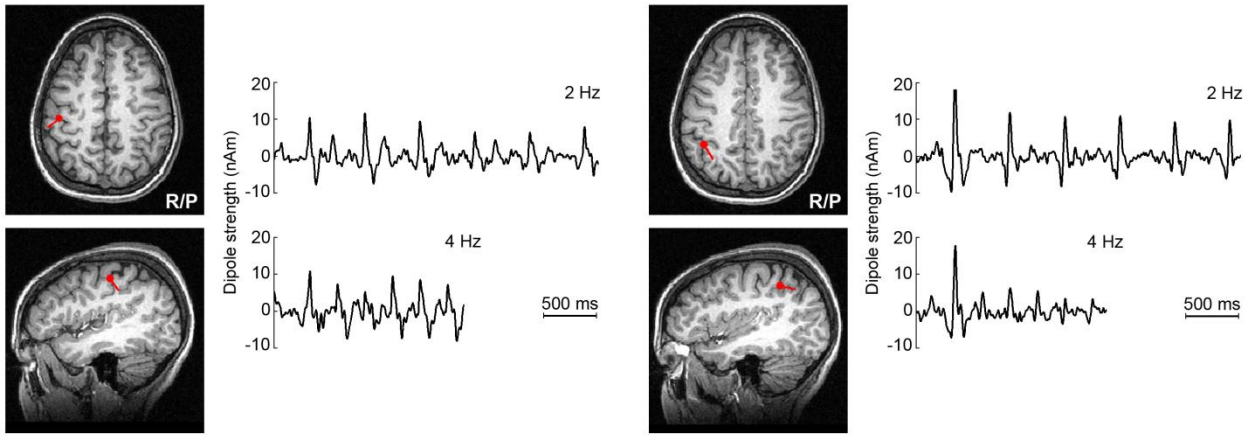

PEAK RESPONSE AMPLITUDE

Figure 20 and 21 shows the mean peak amplitudes for each pulse-index number as a function of stimulus frequency, stimulus site, and the response component for face and hand stimulation respectively. The peak dipole strengths of SI and PPC (for hand stimulation) attenuate rapidly

with each stimulus pulse-index number. The PPC responses exhibit a more pronounced decay of the peak dipole amplitude when compared to SI responses for both 2 and 4 Hz (Figure 21). An ANOVA was performed on the peak response amplitude (dependent variable) for each response component (SI, PPC), stimulation frequency (2 Hz, 4 Hz), stimulus site, and pulse-index number. Significant main effects of stimulation frequency ($F=5.01$, $p=.026$), response component ($F=23.12$, $p<.0001$), and pulse-index number ($F=13.00$, $p<.0001$) were observed. There were no significant interaction effects.

Maximum attenuation in peak response amplitude generally occurs in the response corresponding to the second pulse-index. Further decay is observed for the consequent pulse-index numbers but the observed attenuation is comparatively smaller. For the face stimulation, the peak response has slightly higher amplitude during the third pulse-index when compared to the second pulse-index (Figure 20). Some studies have reported response suppression at the population level (Angel et al., 1985; Tomberg et al., 1989) or in single upper-layer cortical neurons (Lee and Whitsel, 1992), while a similar oscillatory behavior with the serial position subsequent to the second response in the train was also reported by (Angel et al., 1985), and more recently in our in our study using a different type of cutaneous stimulus (Popescu et al., 2010).

Figure 20: Peak dipole strength adaptation in SI for face stimulation.

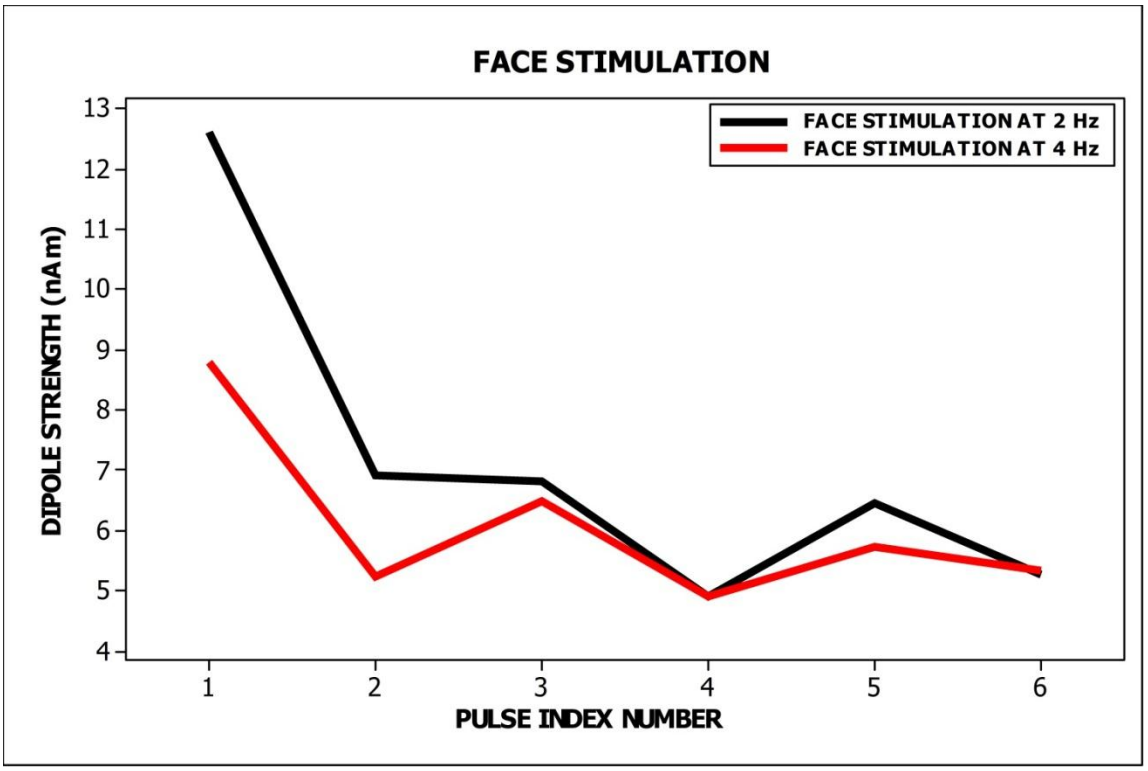

Figure 21: Peak dipole strength adaptation in SI and PPC for hand stimulation.

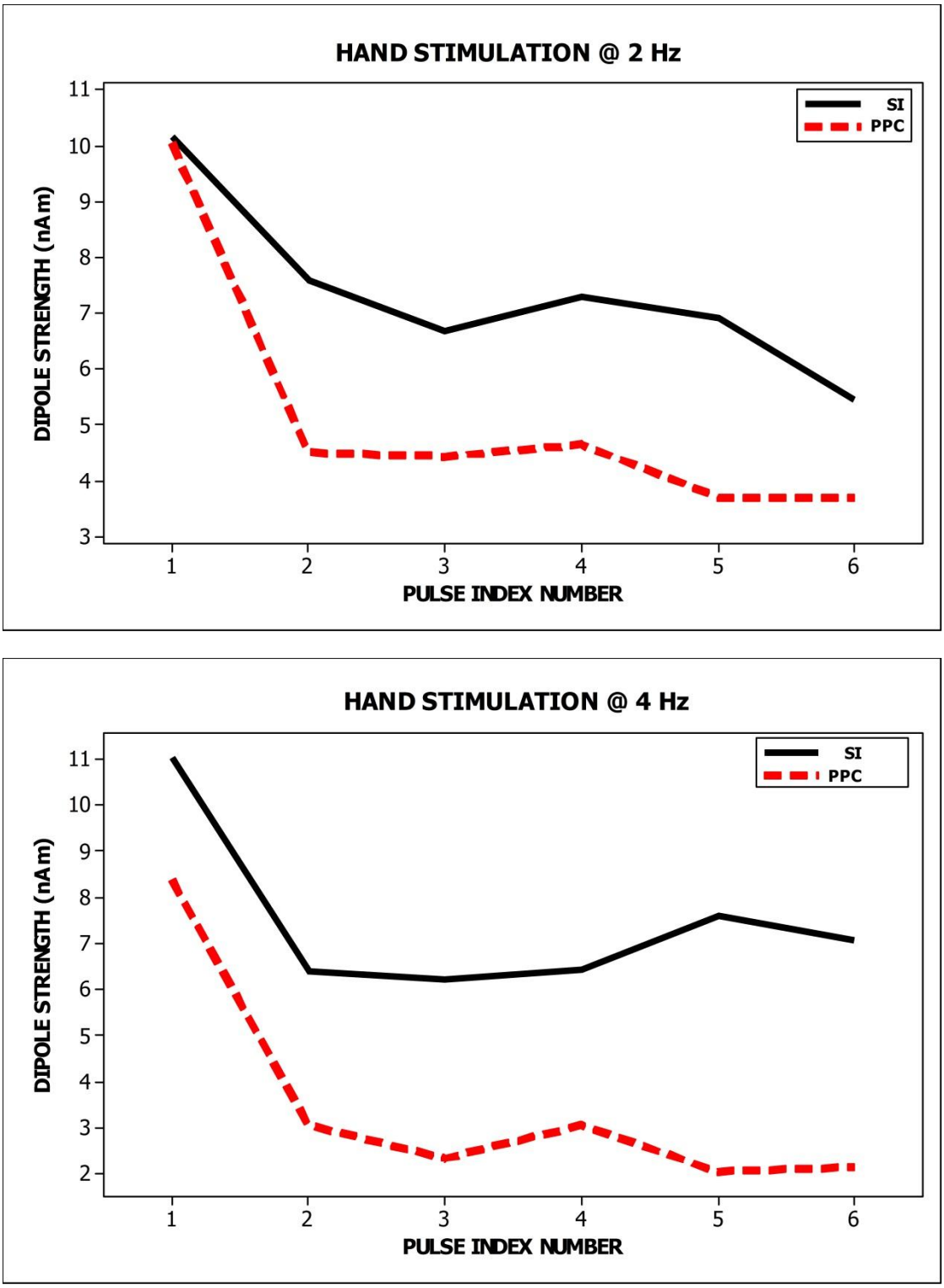

PEAK RESPONSE LATENCY

To test for the presence of stimulation rate- and brain area- dependent adaptation effects on the response latency, an ANOVA was performed, with stimulation frequency (2 Hz, 4 Hz), stimulation site (face, hand), response component (SI, PPC), and pulse-index number (1,2,3,4,5,6) as independent variables, and the peak response latency as dependent variable. Results indicate a significant main effect of the response component ($F=551.05$, $p<.0001$), and stimulation site ($F=201.22$, $p<.0001$). There were significant interaction effects of stimulation frequency and stimulation site ($F=5.00$, $p=.027$), and stimulation frequency and response component ($F=4.00$, $p=.047$). There was no pulse-index- number specific adaptation of the SI, or PPC response latencies. Peak response latencies for each individual component for face and hand stimulation are summarized in Tables 2 and 3 respectively.

Table 2: SI source locations and latencies for face stimulation

Source	**Location (mm)**			**Peak latency (ms)**
	x (right-left)	**y** (posterior-anterior)	**z** (inferior-superior)	
SI	-38 ± 7	5 ± 5	73 ± 9	52 ± 6

Table 3: SI, PPC source locations and latencies for hand stimulation.

Source	Location (mm)			Peak latency (ms)
	x (right-left)	**y** (posterior-anterior)	**z** (inferior-superior)	
SI	-41 ± 5	1 ± 8	84 ± 6	66 ±6
PPC	-37 ± 6	-3 ± 12	86 ± 7	96 ±6

SPECIFIC AIM #2

VIBROTACTILE DETECTION THRESHOLDS

A four-way ANOVA revealed that vibrotactile detection thresholds were significantly dependent on stimulus site ($F=124.80$, $p<.0001$), sex ($F=23.18$, $p<.0001$), and frequency of stimulation ($F=121.03$, $p<.0001$). There was significant interaction between age and stimulus site ($F=3.19$, $p=.042$), age and frequency of stimulation ($F=2.60$, $p=.024$), and stimulation site and frequency of stimulation ($F=11.53$, $p<.0001$). Further analysis showed that the vibration detection thresholds were significantly higher for the older-adults (Figure 23) at all frequencies for finger stimulation ($F=14.85$, $p<.0001$), but not for cheek or lip stimulation. VDT was highest for cheek stimulation followed by lip and finger stimulation (Figure 22). In general, VDT decreases as frequency increases, and the VDT's illustrate the Pacinian type-response at 250 and 300 Hz. Males have significantly higher VDT's than females at all frequencies but the difference decreases at higher frequencies (Figure 24).

Figure 22: Comparison of Vibrotactile Detection Thresholds (VDT) between the 3 stimulation sites.

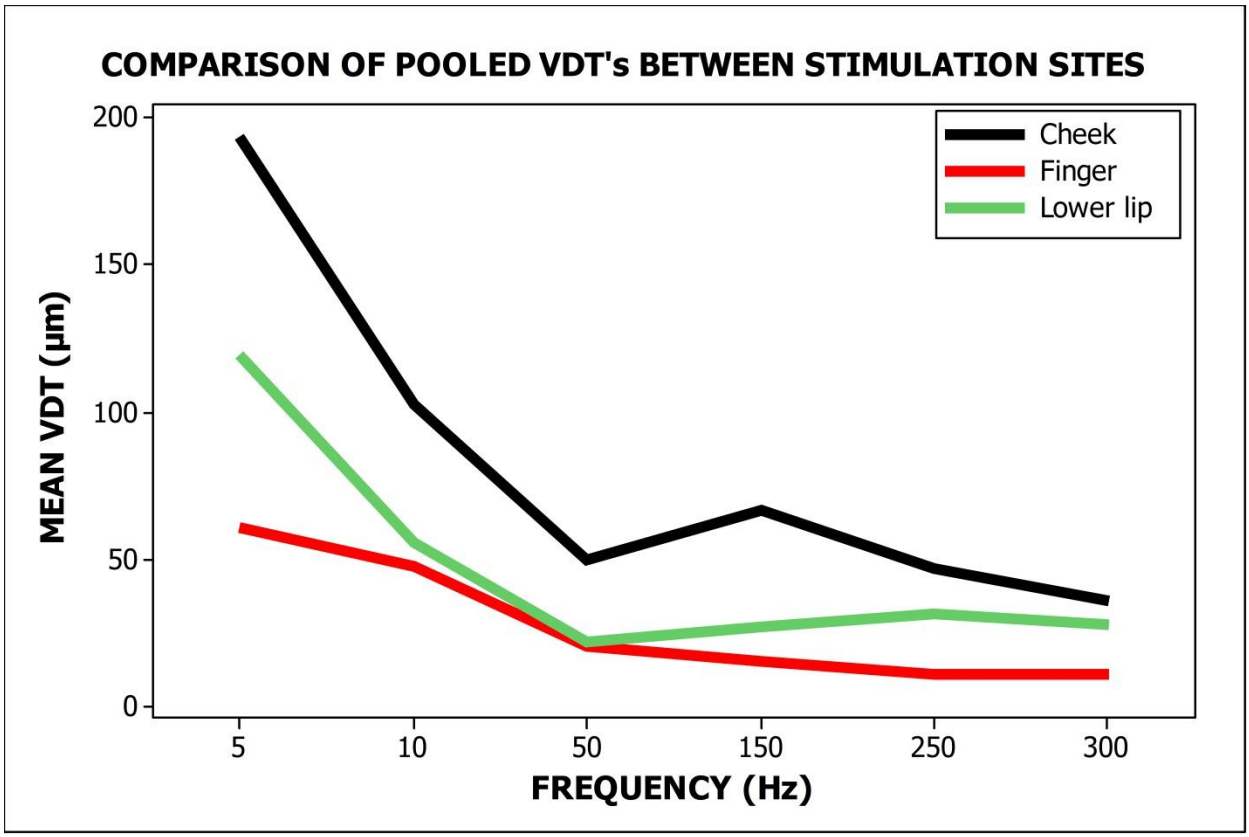

Figure 23: Comparison of Vibrotactile Detection Thresholds (VDT) between younger and older adults.

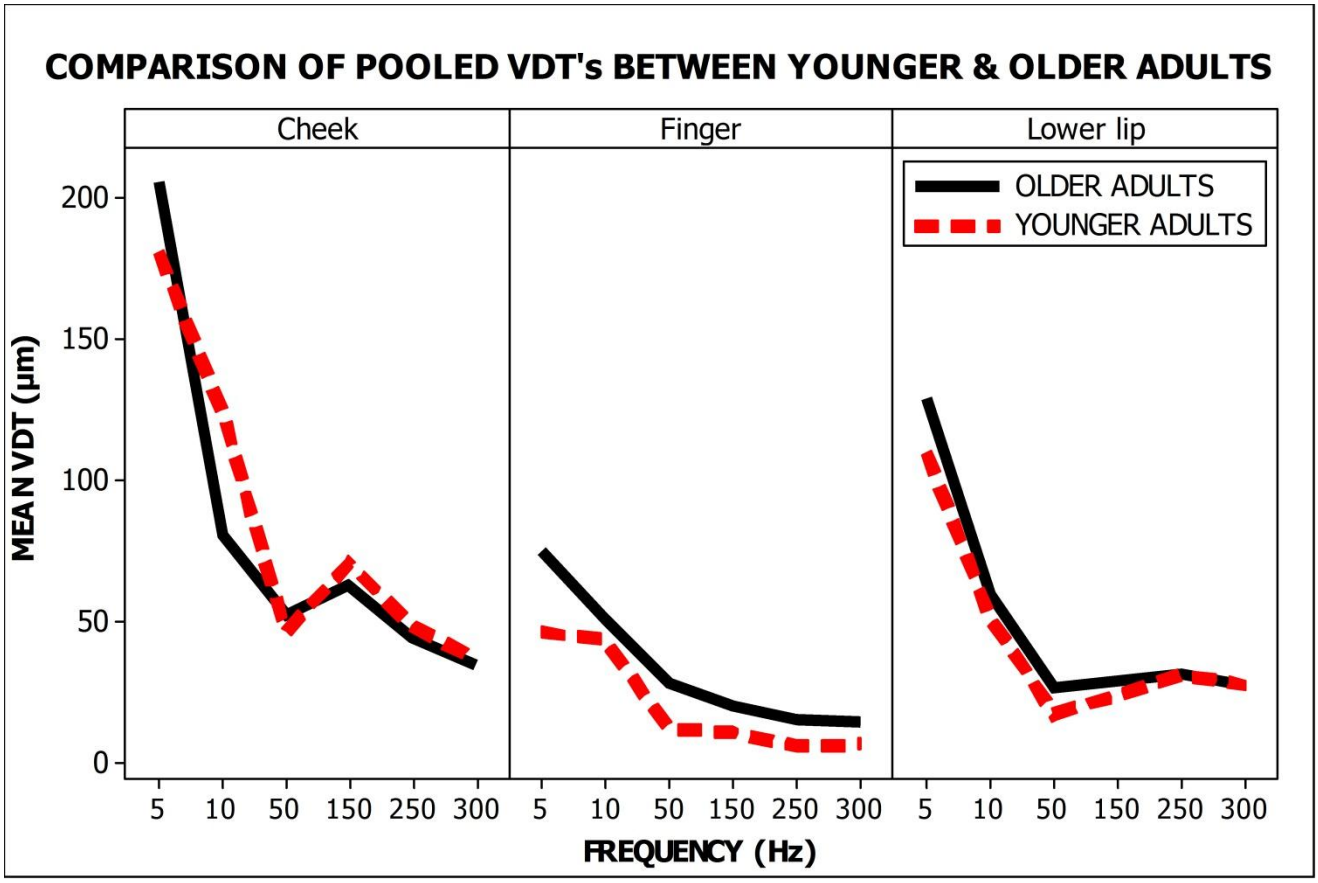

Figure 24: Comparison of Vibrotactile Detection Thresholds (VDT) between males and females.

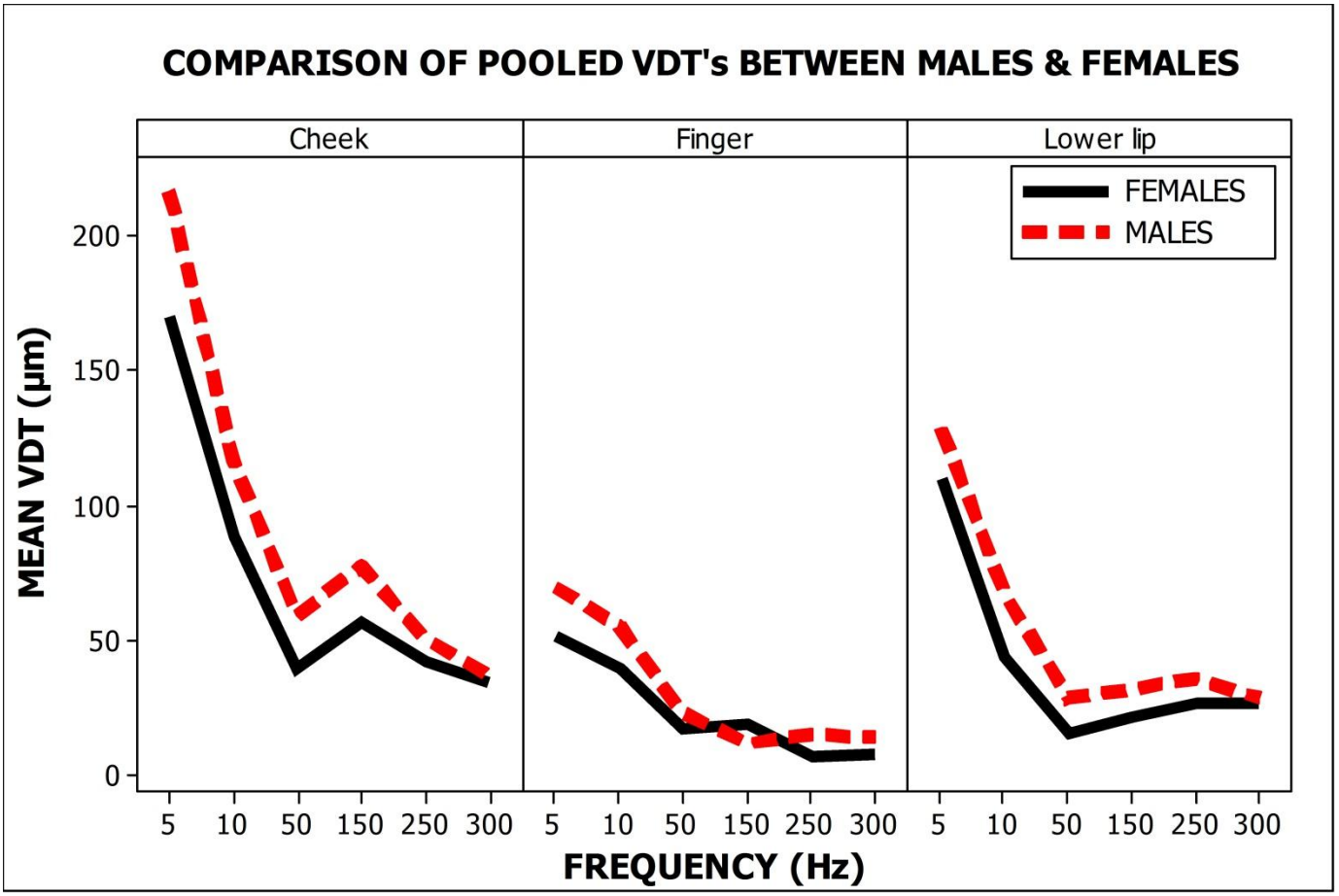

SPECIFIC AIM #3

DISPLACEMENT PEAKS

The displacement peaks at the finger due to TAC-Cell stimulation are significantly dependent on the sex of the participant ($F=279.71$, $p<.0001$) for all motor inputs ($F=542.97$, $p<.0001$) (Figure 25). The average displacement peak values for both males and females are shown in Table 4.

Figure 25: Comparison of mean displacement peaks between males and females.

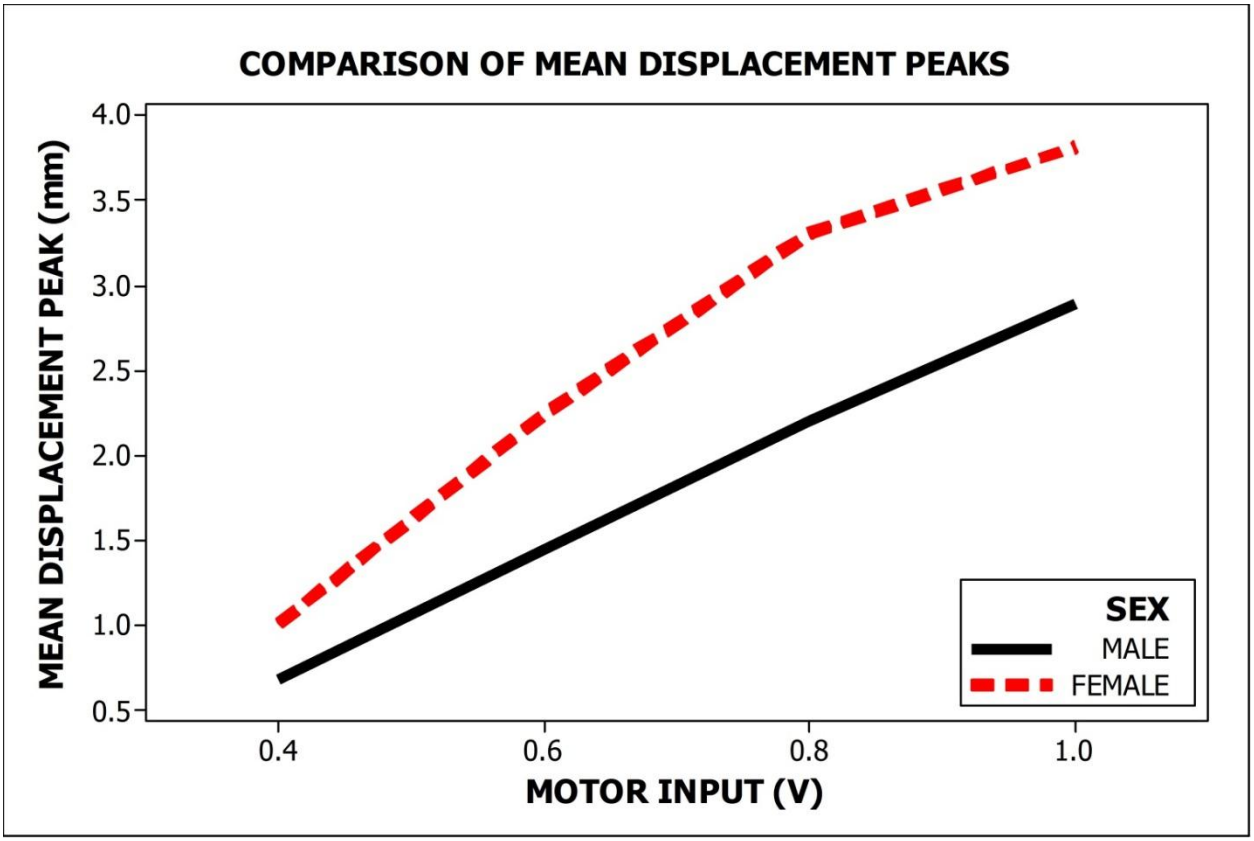

STIMULUS PRESSURE

Stimulus pressure is controlled by the motor-input. Stimulus pressure increases as motor-input increases (Figure 26), and is comparable between males and females (Table 4) for corresponding motor inputs. Average stimulus pressure peak values for both males and females are shown in Table 4.

Figure 26: Comparison of mean stimulus pressure peaks between males and females**.**

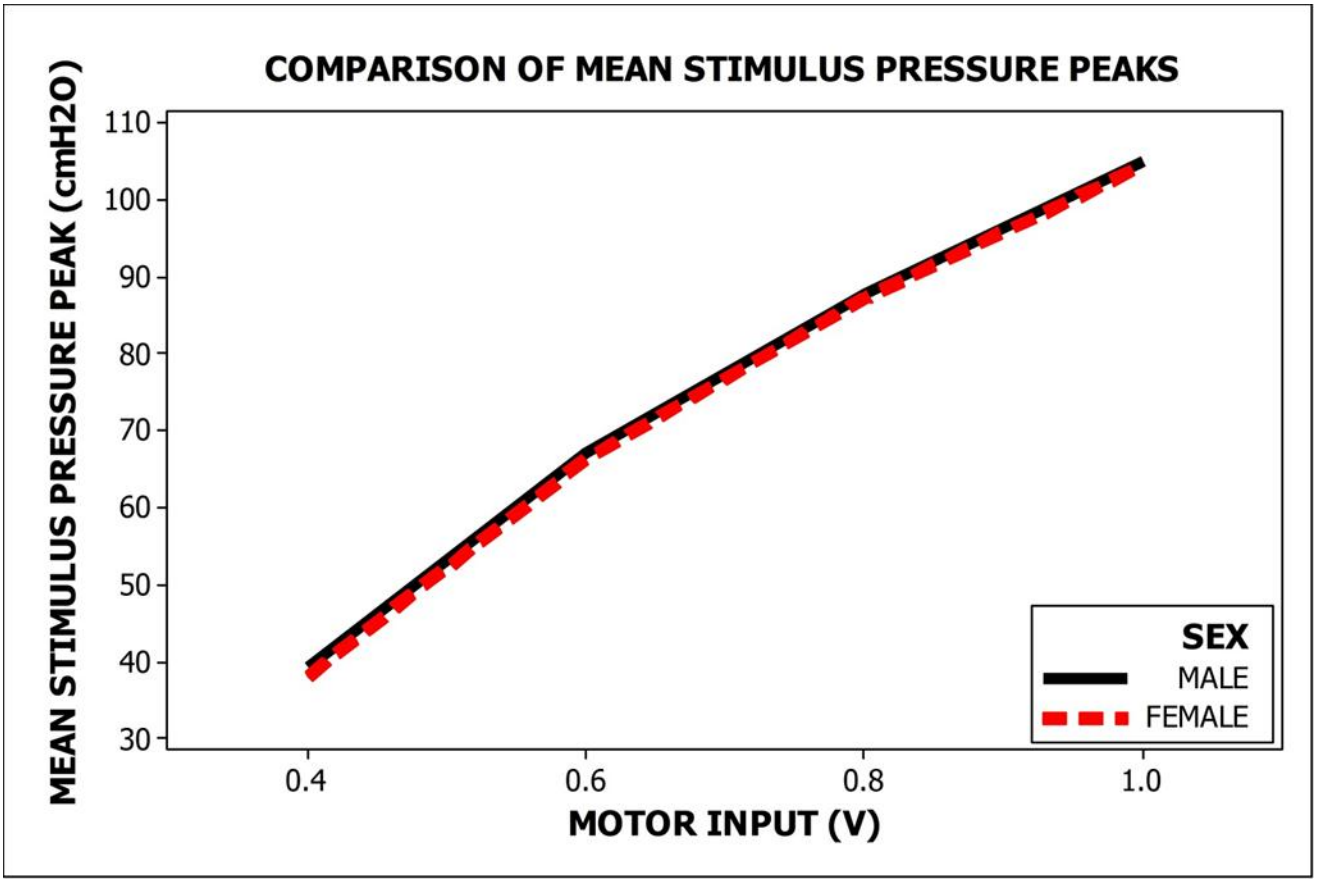

Table 4: Mean displacement peaks, stimulus pressure peaks, and 10-90% rise & fall times**.**

Sex	Motor Input (V)	Displacement Peak (mm) Mean ± SD	Stimulus Pressure Peak (cmH2O) Mean ± SD	10-90% Rise Times (ms) Mean ± SD	10-90% Fall Times (ms) Mean ± SD
Females	1.0	3.82 ± 0.63	104.60 ± 2.14	15.30 ± 1.95	14.65 ± 2.92
	0.8	3.31 ± 0.68	87.30 ± 1.18	15.45 ± 2.12	13.18 ± 2.73
	0.6	2.24 ± 0.75	66.40 ± 1.09	13.37 ± 1.60	15.80 ± 3.21
	0.4	1.00 ± 0.50	38.25 ±1.26	8.45 ± 1.30	22.41 ± 3.86
Males	1.0	2.90 ± 0.82	105.08 ± 2.20	19.44 ± 3.01	14.81 ± 3.17
	0.8	2.20 ± 0.70	87.85 ± 1.23	18.28 ± 2.21	15.01 ± 3.83
	0.6	1.45 ± 0.50	67.09 ± 1.13	13.7 ± 1.70	17.57 ± 3.30
	0.4	0.67 ± 0.28	39.32 ± 1.02	8.49 ± 1.30	24.4 ± 5.49

POWER SPECTRUM ANALYSIS

Power spectrums were calculated for displacement and stimulus pressure peaks for different motor inputs to compare the amplitude and distribution of the spectra between male and female participants. Displacement peak power spectrums for females were noticeably higher when compared to males (Figure 29 - 32) but the pressure peak power spectrums were comparable between the two groups (Figure 35 - 38). The energy in the displacement and pressure peak power spectrums is higher for larger motor inputs (Figure 27, 28, 33, and 34).

Figure 27: Displacement Peak Power Spectrum comparison for different stimulus amplitudes in males.

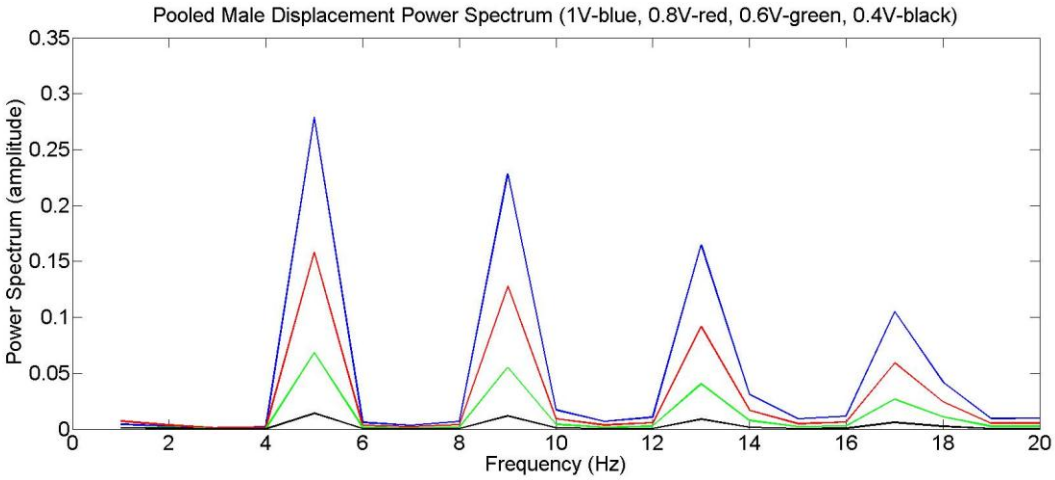

Figure 28: Displacement Peak Power Spectrum comparison for different stimulus amplitudes in females

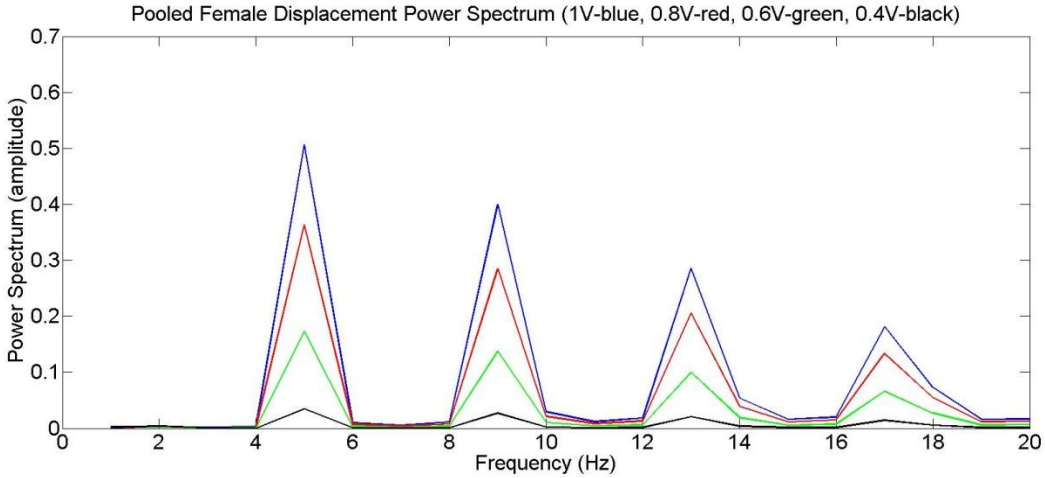

Figure 29: Displacement Peak Power Spectrum comparison between males and females when motor input = 1V

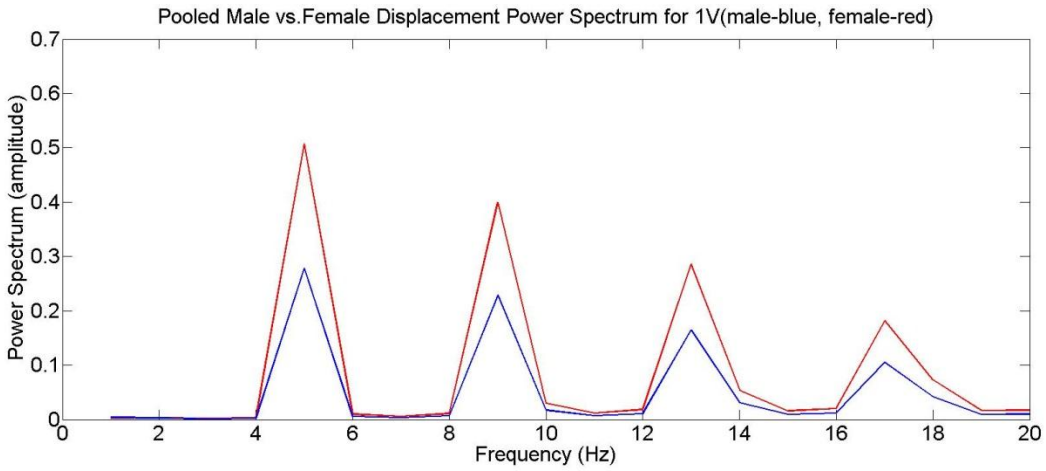

Figure 30: Displacement Peak Power Spectrum comparison between males and females when motor input = 0.8V

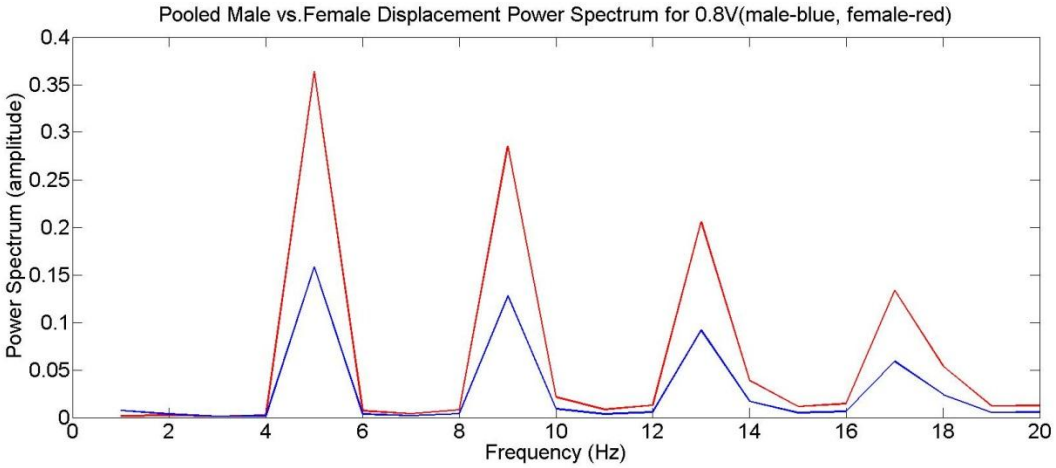

Figure 31: Displacement Peak Power Spectrum comparison between males and females when motor input = 0.6V

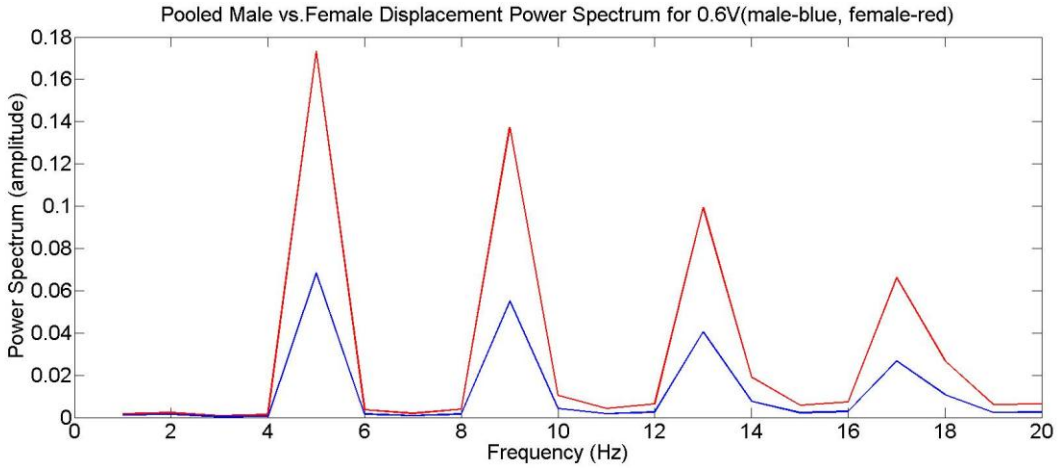

Figure 32: Displacement Peak Power Spectrum comparison between males and females when motor input = 0.4V

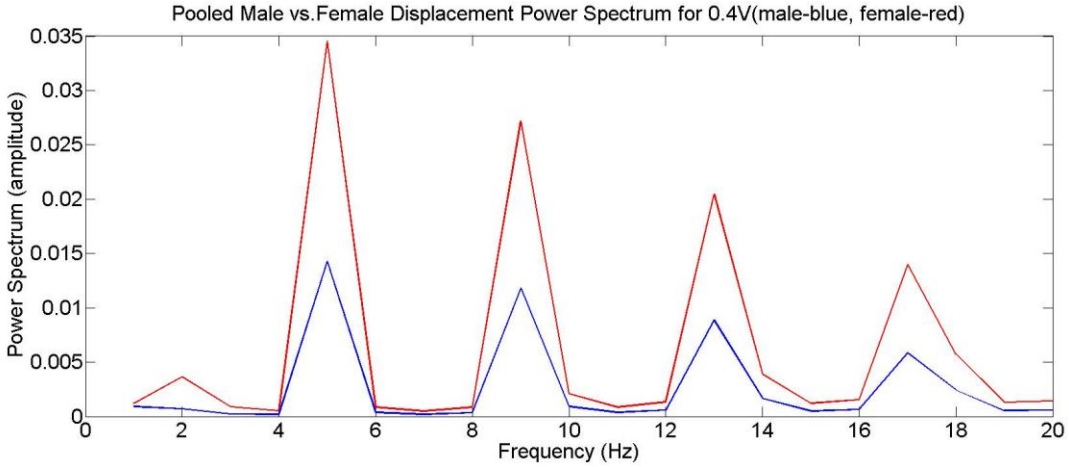

Figure 33: Stimulus Pressure Peak Power Spectrum comparison for different motor inputs in males

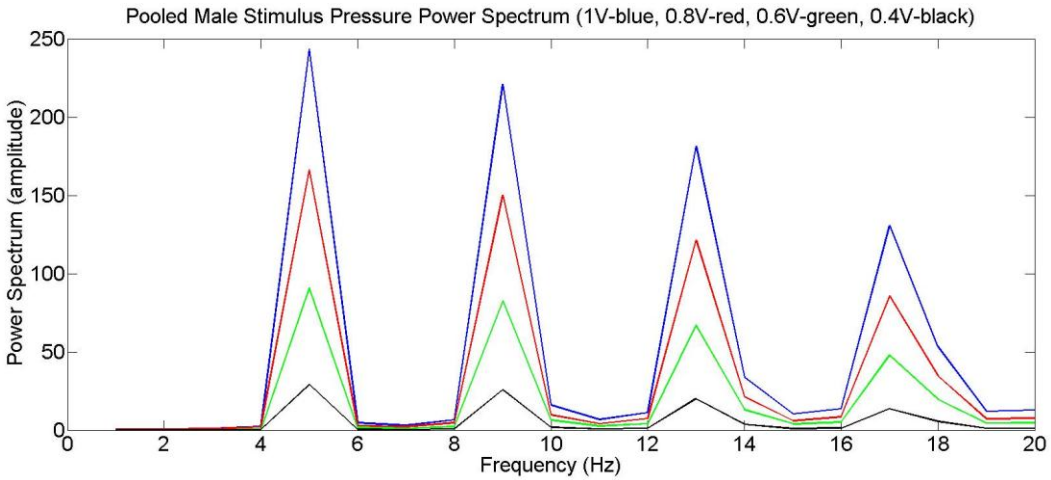

Figure 34: Stimulus Pressure Peak Power Spectrum comparison for different motor inputs in females

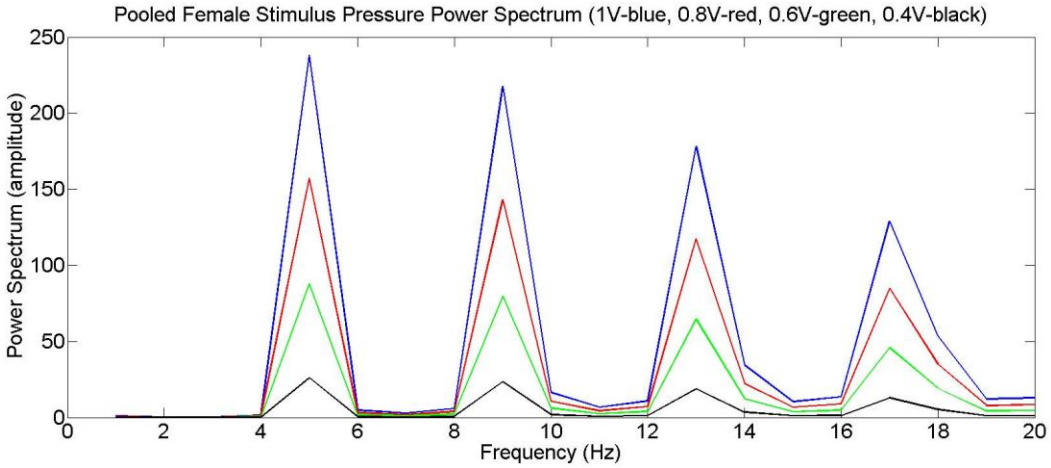

Figure 35: Stimulus Pressure Peak Power Spectrum comparison between males and females when motor input = 1V

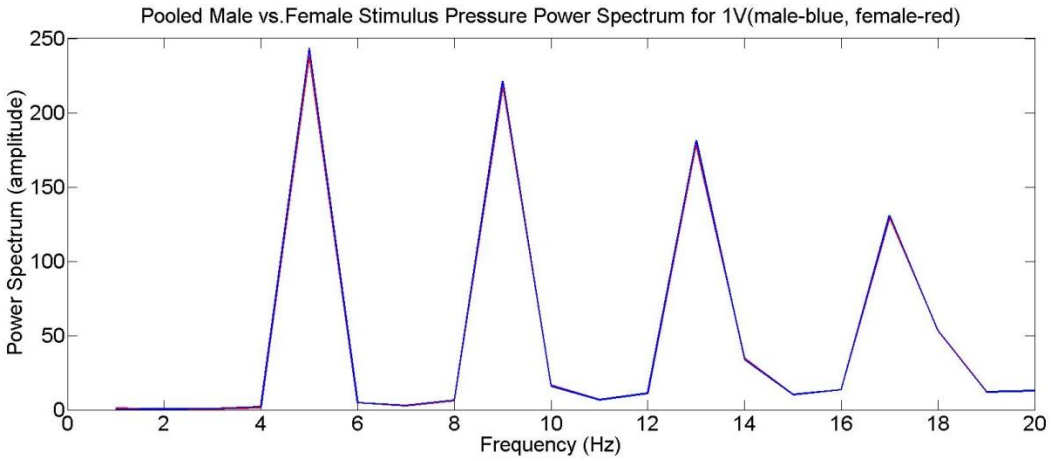

Figure 36: Stimulus Pressure Peak Power Spectrum comparison between males and females when motor input = 0.8V

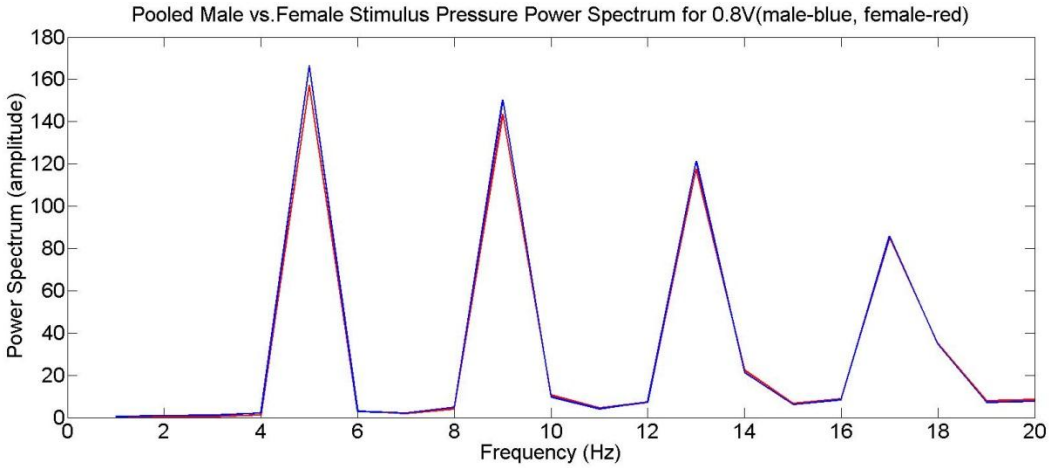

Figure 37: Stimulus Pressure Peak Power Spectrum comparison between males and females when motor input = 0.6V

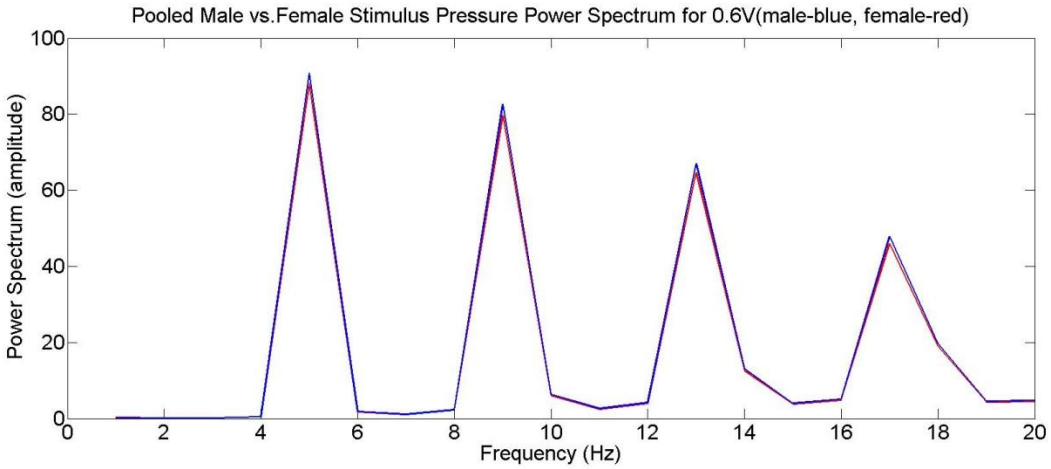

Figure 38: Stimulus Pressure Peak Power Spectrum comparison between males and females when motor input = 0.4V

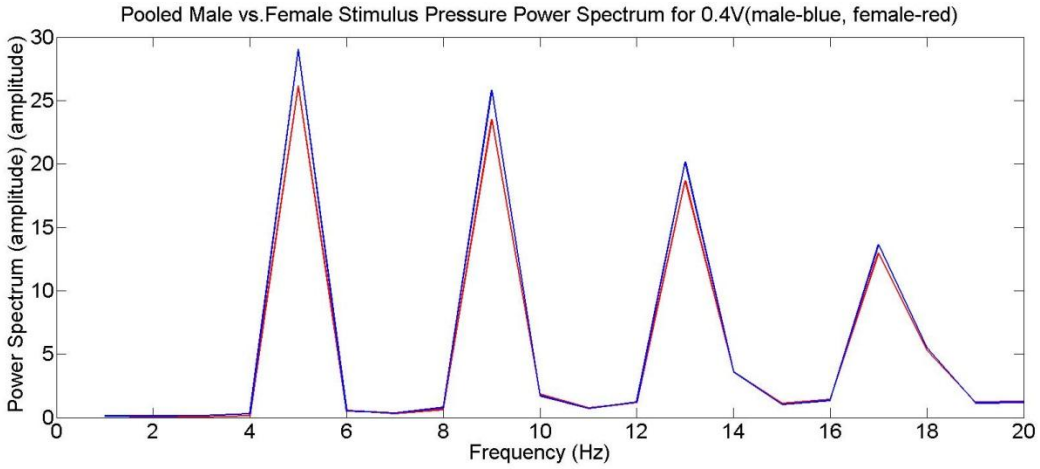

CHAPTER FOUR: DISCUSSION

SPECIFIC AIMS DISCUSSION

AIM #1

Electrical stimulation of the peripheral afferent nerves could result in a highly-replicable cortical response. However, stimulation using this modality bypasses the sensory receptors of the skin, entrains undifferentiated afferents, and generates "unnatural" interactions at subcortical and cortical levels (Willis and Coggeshall, 1991). Mechanical stimulation of the facial region in the MEG environment presents technical challenges due to electrical interference produced by devices like piezoelectric crystals, linear motors and actuators, or the added challenge of signal spread, calibration and tedious setup associated with air-puff stimuli.

The MEG/MRI compatible TAC-Cell developed in our laboratory was highly effective in activating the somatosensory cortex in healthy adult participants (Venkatesan et al., 2010). The newer, smaller TAC-Cell used in this study is highly efficient in producing a controlled, inaudible stimulus, and has the capability to displace the skin any stimulation site to produce an adequate cortical response.

Repetitive patterned pneumatic stimulation of the hand and face using the mini-TAC-Cells evoked responses in SI and somatosensory association areas like PPC (only for hand stimulation). This allowed for a comparison of the characteristics of cortical adaptation in multiple-levels of the somatosensory cortical network.

RESPONSE LOCATIONS

Many experimental studies have shown that the PPC plays a role in multimodal stimulus integration, e.g. audiotactile stimulus processing (Gobbele et al., 2003), and during visual-manual exploration tasks like grasp, self-feeding behaviors, and coordinated motor tasks that involve the hands (Fogassi et al., 2005; Hinkley et al., 2009; Hyvarinen, 1982). Activity in the PPC has also been observed during median nerve (Forss et al., 1994), vibrotactile (Bardouille and Ross, 2008), and pneumotactile (Popescu et al., 2012) stimulation of the hand. No study to date has shown that the PPC is activated during repetitive passive tactile stimulation of the face. Somatotopic representation of the hand and foot has been observed in the PPC, with the hand area being closer to SI when compared to the foot (Hoshiyama et al., 1997). In the same study, lip stimulation showed no consistent activity in the PPC, leading to the speculation that the lip area might not be represented in the PPC. The absence of PPC response during TAC-Cell stimulation of the face seems to corroborate the idea of the absence of face representation in the PPC.

In contrast, bilateral evoked responses in the ventro-lateral somatosensory association areas (SII) were not clearly identifiable during face or hand stimulation. Suppression of SII activity during hand stimulation was observed in a prior study using the TAC-Cell (Popescu et al., 2012). Significant SII activation was not observed in a similar study that used a pneumatic device to deliver a vibrotactile stimulus to the index finger (Bardouille and Ross, 2008). The nature of the somatosensory stimulus required to activate SII has not fully been understood. Electrical stimulation represents a more unnatural mode of stimulation when compared to delivering a punctate stimulus using the TAC-Cell. Electrical stimulation has resulted in bilateral SII activity (Forss et al., 1994), but it recruits many undifferentiated fibers, and increases the probability of

evoking a response. The large, bilateral receptive fields in SII respond more vigorously to a moving stimulus than a stationary stimulus (Bodegard et al., 2001; Disbrow et al., 2000). A consistent cortical response is observed in the SII when a larger area of the skin is stimulated (e.g., via a rotating brush), or when the task involves sensorimotor integration (e.g. tactile discrimination of roughness, shape, or texture, object manipulation). Repeated stimulation of a small, focal area on the face or finger using a passive stimulator like the TAC-Cell might not be adequate to induce a consistent SII response.

RESPONSE AMPLITUDES

Difference in short-term adaptation patterns of the hand and face may be a function of the difference in mechanoreceptor typing in cutaneous and subcutaneous regions and also due to the difference in facial and limbic musculature. The magnitude of attenuation of SI response depends on the stimulus frequency and pulse index with attenuation being most prominent at higher frequencies for both hand and face stimulation. PPC response amplitudes exhibit a higher sensitivity to repeated stimulation of the hand. This may be due to hierarchy in the SI-PPC network, and the associative areas inheriting the adaptation in SI. PPC is involved in higher-order stimulus processing and has a more complex multisensory receptive field. Higher-levels of adaptation to auditory stimuli have been observed in areas with larger receptive fields (Lu et al., 1992) that are similar to PPC.

RESPONSE LATENCIES

The significant difference between the latencies of peak dipole strengths of hand and lip SI, and hand PPC is attributable to the difference in axon length and distance from the mechanosensory nerve terminals in the lip and hand to their central targets in SI. A short delay in the PPC

response reveals the hierarchy in the serial-processing mechanism that exists in the somatosensory cortical network. These results also reflect the role of the somatosensory association areas in sensorimotor integration. Rapid processing and integration of tactile and proprioceptive data from afferent receptors and muscle spindles is essential for continuous relay of this information to the related motor areas. Continuous sensorimotor feedback is essential for planning and execution of exploratory movements (Lederman and Klatzky, 1987).

AIM #2

STIMULUS SITE

VDT's were significantly different between the 3 stimulus sites (finger, lips, cheek), with the fingers having the lowest thresholds (Figure 22). These results are consistent with previous observations that the type and distribution of mechanoreceptors vary significantly between the finger and face. The net-reactive force produced by skin displacement is higher in glabrous than non-glabrous skin (Pubols, 1982). The net-gain in the reactive force may be responsible for the higher VDT's in the cheek when compared to the lower-lip vermilion.

FREQUENCY

VDT's were significantly dependent on stimulus frequencies for the 3 stimulus sites (Figure 22). This illustrates the presence of four different mechanoreceptors that are recruited differentially to assist in the detection of different vibration frequencies. Pacinian-type sensitivity (at 250 & 300 Hz) is absent in the face due to apparent lack of Pacinian corpuscles.

SEX

VDT's were significantly dependent on sex for the 3 stimulus sites (Figure 24). Tactile detection thresholds of painful stimuli are lower in females when compared to males for cheek (Komiyama and De Laat, 2005; Komiyama et al., 2007), and thumb (Komiyama et al., 2007). An adaptive psychophysical procedure (Chen et al., 1995) calculates the threshold spatial separation for perceiving two points of contact at various sites on the face. This study showed that spatial separation thresholds were lower in both the lip vermilions, and the cheek in female subjects when compared to males. Difference in male and female finger sizes results in a higher density of Meissner's corpuscles (Dillon et al., 2001) and Merkel's disks (Peters et al., 2009). Tactile perception improves with smaller finger sizes, leading to the conclusion that the difference in receptor density accounts for the higher tactile sensitivity in females. Thickness of the stratum corneum in the volar finger-tips is slightly higher in males when compared to females (Fruhstorfer et al., 2000). A force-controlled stimulus causes greater deformation in skin that is more compliant. Receptor activation is proportional to the skin indentation, with stronger responses being elicited by those within the epidermis of more compliant skin (Peters et al., 2009).

AGE

VDT's were significantly dependent on age for the finger stimulation (Figure 23). It has been suggested that age-related loss of nerve fibers or morphological changes in skin can reduce the efficiency of stimulus transmission (Pearce and Grimmer, 1972). Changes in the physical structure of the skin with aging have been characterized by a reduction in the number of cell layers in the stratum spinosum (Montagna, 1965), increased collagen (Verzar, 1963) and elastin

content in the dermis. Although reduction in tactile acuity in fingers with age has been associated with the decrease in Meissner's corpuscles, there is no significant correlation between the reduction in passive touch thresholds and the number of Meissner's corpuscles (Bruce, 1980; Bruce and Sinclair, 1980). Dynamic structure of mechanoreceptor end organs like the Pacinian corpuscles and Meissner's corpuscles undergo a continuous change during the human lifespan. These changes may signify the morphological adaptation due to different functional requirements (e.g., heavy manual labor). Merkel's disks present in the papillary ridges of the glabrous skin and epidermal folds projecting to the corium of non-glabrous skin undergo a reduction in number but not form or structure as they age (Cauna, 1965). Meissner's corpuscles undergo remarkable morphological changes due to partial atrophy during the lifetime of an individual (Cauna, 1965). There was no apparent difference in vibrotactile threshold detection at the thenar eminence at lower-frequencies (< 40 Hz) that activate the non-Pacinian receptors. Age-related changes in density and morphology (Cauna, 1965) have very little effect on the low frequency response of these receptors. The oval-shaped Pacinian corpuscle is the largest mechanoreceptor found in the cutaneous tissue and its end organ consists of fluid-filled concentric lamellae (Cauna and Mannan, 1958). At birth, the capsule is small and has relatively fewer layers of lamellae. During the human lifespan the capsule increases in size and becomes distorted in shape due to the addition of new lamellae around the periphery (Cauna, 1965). In essence, the capsule acts as a high-pass filter that does not permit low-frequency stimulus components to enter the axon, but transmits the high-frequency components (Loewenstein and Mendelson, 1965; Loewenstein and Skalak, 1966; Verrillo, 1979). Higher VDT's in the fingers of older subjects maybe due to the increase in the number of these filters. An alternate hypothesis could ascertain the increase in threshold sensitivity to the decrease in the number of

Pacinian corpuscles due to functional use (Verrillo, 1979). The progressive loss of receptors with age significantly alters the sensitivity of the P-channel, because spatial summation is an exclusive characteristic of the P channel (Gescheider et al., 2004). Loss of receptors causes smaller effects of aging in 3 NP channels because they are nearly independent of spatial summation and thus there is a lack of significant difference in threshold sensitivity of the lip and cheek between older and younger subjects.

AIM #3

Change in motor input (1V, 0.8V, 0.6V, 0.4V) resulted in a proportional change in stimulus pressure peaks (Figure 26). Although stimulus pressure was clearly comparable for both the sexes (see Table 3, Figure 26) at corresponding motor inputs, displacement peaks were higher for females when compared to males (Figure 25). These differences could be due to differences in skin compliance and conformance, sex-differences, and also the subjects' occupation. Viscoelastic properties and thickness of the skin adapts to the functional use of the hand (e.g. manual labor). The amount of skin indentation to a pneumatic stimulus could be related to skin thickness and the use of a *durometer* (measures skin compliance) in future studies would reveal whether the difference in skin displacement between males and females is due to differences in thickness and compliance of the skin.

POWER SPECTRUM ANALYSIS

Power spectrum analysis of the displacement and pressure peaks reveals a spectrally-rich signal with a clearly-visible fundamental frequency and several harmonics with significant energy. The signal consists of a broad power spectrum with complex harmonic energy up to 20 Hz. The spectral energy in these high frequency components contribute to the high-velocity signal,

making it sufficient enough to activate the medial-lemniscus and trigeminal pathways. Higher displacement peak power for all motor inputs (1V, 0.8V, 0.6V, 0.4V) in females indicates greater skin displacement amplitudes than males.

FUTURE STUDIES

In future studies, examination of correlation between the peak dipole strength amplitudes of the cortical response and the VDT's of the corresponding stimulation sites could prove interesting. Using the skin displacement data obtained through the fiber-optic sensors, the TAC-Cell stimulus pressure could be modified such that the skin overlying the stimulation site in every participant is displaced by the same extent. Cortical responses obtained for those TAC-Cell inputs could provide for an interesting comparison.

Comparison of the spatiotemporal adaptation patterns and VDT's between normal healthy adults and different clinical populations such as children with autism, adults with a traumatic brain injury or a cerebrovascular stroke may shed new insight on fundamental sensory processes. For example, repeated tactile stimulation in children with autism resulted in hypersensitivity (Blakemore et al., 2006), and an enhanced but slower adaptation response (Baranek and Berkson, 1994; Baranek et al., 1997). A suppressed GABAergic inhibition mechanism (Hussman, 2001) due to the reduction in the proteins utilized for synthesizing GABA (Fatemi et al., 2002) is believed to be responsible for these abnormal response characteristics. New findings have demonstrated significant impairments in somatosensory function in individuals with autism, including altered central representations of somatosensory function (Coskun et al., 2009), degraded tactile spatial localization following inputs to the glabrous hand (Teitelbaum et al., 1998), abnormal multisensory integration (auditory-somatosensory) (Russo et al., 2010), brain asymmetry in processing somatosensory tactile inputs (Wittling et al., 2009), and cortical

hyperactivity in response to median nerve stimulation using a classic evoked potential paradigm (Miyazaki et al., 2007). Altered somatosensory signal detection and discrimination processes are presumed to impact a wide range of perceptual mechanisms and behavior. There might be a significant correlation between the neuromagnetic MEG response, VDT's, and heightened sensory responsiveness in people with autism when compared with normal individuals.

Studies suggest that a common neural architecture underlies sensory input processing and motor output control, and a potential role for perception in motor development and rehabilitation (Meegan et al., 2000). Sustained somatosensory stimulation can increase motor cortex excitability (Luft et al., 2002) and has implications in motor learning and recovery of function in humans with cortical lesions or movement disorders (Conforto et al., 2002; Kaelin-Lang et al., 2002). Tactile electrical stimulation has proved to be beneficial during stroke rehabilitation, but shows no significant long-term improvement. Little is known about the effect of patterned tactile cutaneous stimulation of the paretic side of the body during rehabilitation. Patterned, natural cutaneous somatosensory stimulation temporally matched to target movement can substitute for motor training (Meegan et al., 2000; Planetta and Servos, 2008) in systems where neural control of movement is either underdeveloped or impaired. The TAC-Cell Array that is being developed at our laboratory (Communication Neuroscience Laboratory, KU) can be programmed to produce apparent motion that imitates select kinematic features (timing, velocity, direction, spatial information) of target movement (e.g., speech, manipulation, grasp) and has considerable potential as a neurotherapeutic intervention in movement disorders.

Clinical tests of direction discrimination are particularly sensitive to injuries to the sensory branches of the trigeminal nerve (Bailey and Bays, 1984; Nishioka et al., 1987; Walter and Gregg, 1979; Zaytoun et al., 1986) than other sensory measures. Integrity of dorsal columns is

required for normal direction discrimination in non-human primates (Vierck, 1974; Vierck et al., 1983) and humans (Hankey and Edis, 1989). Neurological testing of direction discrimination may assist in assessing the extent of spinal cord injuries. Thus, the TAC-Cell Array could also be used for basic neurologic assessment of the integrity of trigemino-thalamo-cortical (face) and dorsal column-medial lemniscal-thalamo-cortical (hand-forelimb/foot-hindlimb) somatosensory pathways in human brain.

REFERENCES

Abbott, L.F., Varela, J.A., Sen, K., Nelson, S.B., 1997. Synaptic depression and cortical gain control. Science. 275**,** 220-4.

Andreatta, R.D., Barlow, S.M., 2003. Movement-related modulation of vibrotactile detection thresholds in the human orofacial system. Exp Brain Res. 149**,** 75-82.

Andreatta, R.D., Davidow, J.H., Scott, A.T., 2003. Low-level static lip force control does not alter vibrotactile detection thresholds in the human orofacial system. Exp Brain Res. 151**,** 548-52.

Andreatta, R.D., Davidow, J.H., 2006. Mechanical frequency and stimulation-site-related differences in vibrotactile detection capacity along the lip vermilion in young adults. Clin Oral Investig. 10**,** 17-22.

Andreatta, R.D., Barlow, S.M., 2009. Somatosensory gating is dependent on the rate of force recruitment in the human orofacial system. J Speech Lang Hear Res. 52**,** 1566-78.

Angel, R.W., Quick, W.M., Boylls, C.C., Weinrich, M., Rodnitzky, R.L., 1985. Decrement of somatosensory evoked potentials during repetitive stimulation. Electroencephalogr Clin Neurophysiol. 60**,** 335-42.

Arezzo, J.C., Vaughan, H.G., Jr., Legatt, A.D., 1981. Topography and intracranial sources of somatosensory evoked potentials in the monkey. II. Cortical components. Electroencephalogr Clin Neurophysiol. 51**,** 1-18.

Bailey, P.H., Bays, R.A., 1984. Evaluation of long-term sensory changes following mandibular augmentation procedures. J Oral Maxillofac Surg. 42**,** 722-7.

Baranek, G.T., Berkson, G., 1994. Tactile defensiveness in children with developmental disabilities: responsiveness and habituation. J Autism Dev Disord. 24**,** 457-71.

Baranek, G.T., Foster, L.G., Berkson, G., 1997. Tactile defensiveness and stereotyped behaviors. Am J Occup Ther. 51**,** 91-5.

Bardouille, T., Ross, B., 2008. MEG imaging of sensorimotor areas using inter-trial coherence in vibrotactile steady-state responses. Neuroimage. 42**,** 323-31.

Barlow, S.M., 1987. Mechanical frequency detection thresholds in the human face. Exp Neurol. 96**,** 253-61.

Barlow, S.M., 1998. Real time modulation of speech--orofacial motor performance by means of motion sense. J Commun Disord. 31**,** 511-33; quiz 533-4; 553.

Binkofski, F., Buccino, G., Posse, S., Seitz, R.J., Rizzolatti, G., Freund, H., 1999. A fronto-parietal circuit for object manipulation in man: evidence from an fMRI-study. Eur J Neurosci. 11**,** 3276-86.

Bodegard, A., Geyer, S., Grefkes, C., Zilles, K., Roland, P.E., 2001. Hierarchical processing of tactile shape in the human brain. Neuron. 31**,** 317-28.

Bolanowski, S.J., Gescheider, G.A., Verrillo, R.T., 1994. Hairy skin: psychophysical channels and their physiological substrates. Somatosens Mot Res. 11**,** 279-90.

Bolanowski, S.J., Jr., Gescheider, G.A., Verrillo, R.T., Checkosky, C.M., 1988. Four channels mediate the mechanical aspects of touch. J Acoust Soc Am. 84**,** 1680-94.

Brenner, N., Bialek, W., de Ruyter van Steveninck, R., 2000. Adaptive rescaling maximizes information transmission. Neuron. 26**,** 695-702.

Bruce, M.F., 1980. The relation of tactile thresholds to histology in the fingers of elderly people. J Neurol Neurosurg Psychiatry. 43**,** 730-4.

Bruce, M.F., Sinclair, D.C., 1980. The relationship between tactile thresholds and histology in the human finger. J Neurol Neurosurg Psychiatry. 43**,** 235-42.
Burton, H., Fabri, M., Alloway, K., 1995. Cortical areas within the lateral sulcus connected to cutaneous representations in areas 3b and 1: a revised interpretation of the second somatosensory area in macaque monkeys. J Comp Neurol. 355**,** 539-62.
Burton, H., Snyder, A.Z., Conturo, T.E., Akbudak, E., Ollinger, J.M., Raichle, M.E., 2002. Adaptive changes in early and late blind: a fMRI study of Braille reading. J Neurophysiol. 87**,** 589-607.
Cauna, N., Mannan, G., 1958. The structure of human digital pacinian corpuscles (corpus cula lamellosa) and its functional significance. J Anat. 92**,** 1-20.
Cauna, N., 1965. The effects of aging on the receptors organs of the human dermis. In Advances in Biology of Skin. Vol. VI, W. Montagna, ed.^eds. Pergamon Press, New York, NY, pp. 63-96.
Chen, C.C., Essick, G.K., Kelly, D.G., Young, M.G., Nestor, J.M., Masse, B., 1995. Gender-, side- and site-dependent variations in human perioral spatial resolution. Arch Oral Biol. 40**,** 539-48.
Chu, S.Y., Barlow, S.M., Kieweg, D., Lee, J., 2010. OroSTIFF: Face-referenced measurement of perioral stiffness in health and disease. J Biomech. 43**,** 1476-82.
Chung, S., Li, X., Nelson, S.B., 2002. Short-term depression at thalamocortical synapses contributes to rapid adaptation of cortical sensory responses in vivo. Neuron. 34**,** 437-46.
Conforto, A.B., Kaelin-Lang, A., Cohen, L.G., 2002. Increase in hand muscle strength of stroke patients after somatosensory stimulation. Ann Neurol. 51**,** 122-5.
Connor, N.P., Abbs, J.H., 1998. Orofacial proprioception: analyses of cutaneous mechanoreceptor population properties using artificial neural networks. J Commun Disord. 31**,** 535-42; 553.
Coskun, M.A., Varghese, L., Reddoch, S., Castillo, E.M., Pearson, D.A., Loveland, K.A., Papanicolaou, A.C., Sheth, B.R., 2009. How somatic cortical maps differ in autistic and typical brains. Neuroreport. 20**,** 175-9.
Davidson, P.R., Wolpert, D.M., 2005. Widespread access to predictive models in the motor system: a short review. J Neural Eng. 2**,** S313-9.
Delorme, A., Makeig, S., 2004. EEGLAB: an open source toolbox for analysis of single-trial EEG dynamics including independent component analysis. J Neurosci Methods. 134**,** 9-21.
Dillon, Y.K., Haynes, J., Henneberg, M., 2001. The relationship of the number of Meissner's corpuscles to dermatoglyphic characters and finger size. J Anat. 199**,** 577-84.
Disbrow, E., Roberts, T., Krubitzer, L., 2000. Somatotopic organization of cortical fields in the lateral sulcus of Homo sapiens: evidence for SII and PV. J Comp Neurol. 418**,** 1-21.
Disbrow, E., Roberts, T., Poeppel, D., Krubitzer, L., 2001. Evidence for interhemispheric processing of inputs from the hands in human S2 and PV. J Neurophysiol. 85**,** 2236-44.
Edin, B.B., Abbs, J.H., 1991. Finger movement responses of cutaneous mechanoreceptors in the dorsal skin of the human hand. J Neurophysiol. 65**,** 657-70.
Eickhoff, S.B., Grefkes, C., Zilles, K., Fink, G.R., 2007. The somatotopic organization of cytoarchitectonic areas on the human parietal operculum. Cereb Cortex. 17**,** 1800-11.
Essick, G.K., Afferica, T., Aldershof, B., Nestor, J., Kelly, D., Whitsel, B., 1988. Human perioral directional sensitivity. Exp Neurol. 100**,** 506-23.

Essick, G.K., 1998. Factors affecting direction discrimination of moving tactile stimuli. In Neural aspects of tactile sensation. Vol., J.W. Morley, ed.^eds. Elsevier Science, Amsterdam, pp. 1-54.

Fairhall, A.L., Lewen, G.D., Bialek, W., de Ruyter Van Steveninck, R.R., 2001. Efficiency and ambiguity in an adaptive neural code. Nature. 412**,** 787-92.

Fatemi, S.H., Halt, A.R., Stary, J.M., Kanodia, R., Schulz, S.C., Realmuto, G.R., 2002. Glutamic acid decarboxylase 65 and 67 kDa proteins are reduced in autistic parietal and cerebellar cortices. Biol Psychiatry. 52**,** 805-10.

Felleman, D.J., Van Essen, D.C., 1991. Distributed hierarchical processing in the primate cerebral cortex. Cereb Cortex. 1**,** 1-47.

Fitzgerald, P.J., Lane, J.W., Thakur, P.H., Hsiao, S.S., 2006a. Receptive field (RF) properties of the macaque second somatosensory cortex: RF size, shape, and somatotopic organization. J Neurosci. 26**,** 6485-95.

Fitzgerald, P.J., Lane, J.W., Thakur, P.H., Hsiao, S.S., 2006b. Receptive field properties of the macaque second somatosensory cortex: representation of orientation on different finger pads. J Neurosci. 26**,** 6473-84.

Flanagan, J.R., Bowman, M.C., Johansson, R.S., 2006. Control strategies in object manipulation tasks. Curr Opin Neurobiol. 16**,** 650-9.

Fogassi, L., Ferrari, P.F., Gesierich, B., Rozzi, S., Chersi, F., Rizzolatti, G., 2005. Parietal lobe: from action organization to intention understanding. Science. 308**,** 662-7.

Forss, N., Hari, R., Salmelin, R., Ahonen, A., Hamalainen, M., Kajola, M., Knuutila, J., Simola, J., 1994. Activation of the human posterior parietal cortex by median nerve stimulation. Exp Brain Res. 99**,** 309-15.

Forss, N., Jousmaki, V., 1998. Sensorimotor integration in human primary and secondary somatosensory cortices. Brain Res. 781**,** 259-67.

Friston, K.J., Buechel, C., Fink, G.R., Morris, J., Rolls, E., Dolan, R.J., 1997. Psychophysiological and modulatory interactions in neuroimaging. Neuroimage. 6**,** 218-29.

Fruhstorfer, H., Abel, U., Garthe, C.D., Knuttel, A., 2000. Thickness of the stratum corneum of the volar fingertips. Clin Anat. 13**,** 429-33.

Gabernet, L., Jadhav, S.P., Feldman, D.E., Carandini, M., Scanziani, M., 2005. Somatosensory integration controlled by dynamic thalamocortical feed-forward inhibition. Neuron. 48**,** 315-27.

Gescheider, G.A., Edwards, R.R., Lackner, E.A., Bolanowski, S.J., Verrillo, R.T., 1996. The effects of aging on information-processing channels in the sense of touch: III. Differential sensitivity to changes in stimulus intensity. Somatosens Mot Res. 13**,** 73-80.

Gescheider, G.A., Bolanowski, S.J., Verrillo, R.T., 2004. Some characteristics of tactile channels. Behav Brain Res. 148**,** 35-40.

Gobbele, R., Schurmann, M., Forss, N., Juottonen, K., Buchner, H., Hari, R., 2003. Activation of the human posterior parietal and temporoparietal cortices during audiotactile interaction. Neuroimage. 20**,** 503-11.

Goble, A.K., Hollins, M., 1993. Vibrotactile adaptation enhances amplitude discrimination. J Acoust Soc Am. 93**,** 418-24.

Goble, A.K., Hollins, M., 1994. Vibrotactile adaptation enhances frequency discrimination. J Acoust Soc Am. 96**,** 771-80.

Grafton, S.T., Mazziotta, J.C., Woods, R.P., Phelps, M.E., 1992. Human functional anatomy of visually guided finger movements. Brain. 115 (Pt 2)**,** 565-87.
Hankey, G.J., Edis, R.H., 1989. The utility of testing tactile perception of direction of scratch as a sensitive clinical sign of posterior column dysfunction in spinal cord disorders. J Neurol Neurosurg Psychiatry. 52**,** 395-8.
Hari, R., Reinikainen, K., Kaukoranta, E., Hamalainen, M., Ilmoniemi, R., Penttinen, A., Salminen, J., Teszner, D., 1984. Somatosensory evoked cerebral magnetic fields from SI and SII in man. Electroencephalogr Clin Neurophysiol. 57**,** 254-63.
Hari, R., Karhu, J., Hamalainen, M., Knuutila, J., Salonen, O., Sams, M., Vilkman, V., 1993. Functional organization of the human first and second somatosensory cortices: a neuromagnetic study. Eur J Neurosci. 5**,** 724-34.
Heiss, J.E., Katz, Y., Ganmor, E., Lampl, I., 2008. Shift in the balance between excitation and inhibition during sensory adaptation of S1 neurons. J Neurosci. 28**,** 13320-30.
Hellweg, F.C., Schultz, W., Creutzfeldt, O.D., 1977. Extracellular and intracellular recordings from cat's cortical whisker projection area: thalamocortical response transformation. J Neurophysiol. 40**,** 463-79.
Higley, M.J., Contreras, D., 2006. Balanced excitation and inhibition determine spike timing during frequency adaptation. J Neurosci. 26**,** 448-57.
Hinkley, L.B., Krubitzer, L.A., Padberg, J., Disbrow, E.A., 2009. Visual-manual exploration and posterior parietal cortex in humans. J Neurophysiol. 102**,** 3433-46.
Hironaga, N., Ioannides, A.A., 2007. Localization of individual area neuronal activity. Neuroimage. 34**,** 1519-34.
Hoshiyama, M., Kakigi, R., Koyama, S., Watanabe, S., Shimojo, M., 1997. Activity in posterior parietal cortex following somatosensory stimulation in man: magnetoencephalographic study using spatio-temporal source analysis. Brain Topogr. 10**,** 23-30.
Hsiao, S., 2008. Central mechanisms of tactile shape perception. Curr Opin Neurobiol. 18**,** 418-24.
Hussman, J.P., 2001. Suppressed GABAergic inhibition as a common factor in suspected etiologies of autism. J Autism Dev Disord. 31**,** 247-8.
Huttunen, J., Wikstrom, H., Korvenoja, A., Seppalainen, A.M., Aronen, H., Ilmoniemi, R.J., 1996. Significance of the second somatosensory cortex in sensorimotor integration: enhancement of sensory responses during finger movements. Neuroreport. 7**,** 1009-12.
Hyvarinen, J., 1982. Posterior parietal lobe of the primate brain. Physiol Rev. 62**,** 1060-129.
Iwasaki, T., Goto, N., Goto, J., Ezure, H., Moriyama, H., 2003. The aging of human Meissner's corpuscles as evidenced by parallel sectioning. Okajimas Folia Anat Jpn. 79**,** 185-9.
James, A., Essick, G.K., Kelly, D.G., Tappouni, H., McGlone, F.P., 2000. Frequency and site-dependent variations in vibration detection thresholds on the face. Somatosens Mot Res. 17**,** 349-60.
Jenkins, W.M., Merzenich, M.M., Ochs, M.T., Allard, T., Guic-Robles, E., 1990. Functional reorganization of primary somatosensory cortex in adult owl monkeys after behaviorally controlled tactile stimulation. J Neurophysiol. 63**,** 82-104.
Johansson, R.S., Trulsson, M., Olsson, K.A., Abbs, J.H., 1988a. Mechanoreceptive afferent activity in the infraorbital nerve in man during speech and chewing movements. Exp Brain Res. 72**,** 209-14.
Johansson, R.S., Trulsson, M., Olsson, K.A., Westberg, K.G., 1988b. Mechanoreceptor activity from the human face and oral mucosa. Exp Brain Res. 72**,** 204-8.

Johnson, K.O., Yoshioka, T., Vega-Bermudez, F., 2000. Tactile functions of mechanoreceptive afferents innervating the hand. J Clin Neurophysiol. 17**,** 539-58.
Jones, E.G., Powell, T.P., 1969a. Connexions of the somatic sensory cortex of the rhesus monkey. II. Contralateral cortical connexions. Brain. 92**,** 717-30.
Jones, E.G., Powell, T.P., 1969b. Connexions of the somatic sensory cortex of the rhesus monkey. I. Ipsilateral cortical connexions. Brain. 92**,** 477-502.
Jones, E.G., Powell, T.P., 1970a. An anatomical study of converging sensory pathways within the cerebral cortex of the monkey. Brain. 93**,** 793-820.
Jones, E.G., Powell, T.P., 1970b. Connexions of the somatic sensory cortex of the rhesus monkey. 3. Thalamic connexions. Brain. 93**,** 37-56.
Kaelin-Lang, A., Luft, A.R., Sawaki, L., Burstein, A.H., Sohn, Y.H., Cohen, L.G., 2002. Modulation of human corticomotor excitability by somatosensory input. J Physiol. 540**,** 623-33.
Khalil, Z., Ralevic, V., Bassirat, M., Dusting, G.J., Helme, R.D., 1994. Effects of ageing on sensory nerve function in rat skin. Brain Res. 641**,** 265-72.
Komiyama, O., De Laat, A., 2005. Tactile and pain thresholds in the intra- and extra-oral regions of symptom-free subjects. Pain. 115**,** 308-15.
Komiyama, O., Kawara, M., De Laat, A., 2007. Ethnic differences regarding tactile and pain thresholds in the trigeminal region. J Pain. 8**,** 363-9.
Lauria, G., Holland, N., Hauer, P., Cornblath, D.R., Griffin, J.W., McArthur, J.C., 1999. Epidermal innervation: changes with aging, topographic location, and in sensory neuropathy. J Neurol Sci. 164**,** 172-8.
Lecluyse, W., Meddis, R., 2009. A simple single-interval adaptive procedure for estimating thresholds in normal and impaired listeners. J Acoust Soc Am. 126**,** 2570-9.
Lederman, S.J., Klatzky, R.L., 1987. Hand movements: a window into haptic object recognition. Cogn Psychol. 19**,** 342-68.
Lee, C.J., Whitsel, B.L., 1992. Mechanisms underlying somatosensory cortical dynamics: I. In vivo studies. Cereb Cortex. 2**,** 81-106.
Loewenstein, W.R., Mendelson, M., 1965. Components of Receptor Adaptation in a Pacinian Corpuscle. J Physiol. 177**,** 377-97.
Loewenstein, W.R., Skalak, R., 1966. Mechanical transmission in a Pacinian corpuscle. An analysis and a theory. J Physiol. 182**,** 346-78.
Lu, Z.L., Williamson, S.J., Kaufman, L., 1992. Behavioral lifetime of human auditory sensory memory predicted by physiological measures. Science. 258**,** 1668-70.
Luft, A.R., Kaelin-Lang, A., Hauser, T.K., Buitrago, M.M., Thakor, N.V., Hanley, D.F., Cohen, L.G., 2002. Modulation of rodent cortical motor excitability by somatosensory input. Exp Brain Res. 142**,** 562-9.
Maldjian, J.A., Gottschalk, A., Patel, R.S., Detre, J.A., Alsop, D.C., 1999. The sensory somatotopic map of the human hand demonstrated at 4 Tesla. Neuroimage. 10**,** 55-62.
Manzoni, T., Conti, F., Fabri, M., 1986. Callosal projections from area SII to SI in monkeys: anatomical organization and comparison with association projections. J Comp Neurol. 252**,** 245-63.
Meegan, D.V., Aslin, R.N., Jacobs, R.A., 2000. Motor timing learned without motor training. Nat Neurosci. 3**,** 860-2.

Miyazaki, M., Fujii, E., Saijo, T., Mori, K., Hashimoto, T., Kagami, S., Kuroda, Y., 2007. Short-latency somatosensory evoked potentials in infantile autism: evidence of hyperactivity in the right primary somatosensory area. Dev Med Child Neurol. 49**,** 13-7.
Montagna, W., 1965. The Skin. Sci Am. 212**,** 56-66.
Mountcastle, V.B., Lynch, J.C., Georgopoulos, A., Sakata, H., Acuna, C., 1975. Posterior parietal association cortex of the monkey: command functions for operations within extrapersonal space. J Neurophysiol. 38**,** 871-908.
Muller, J.R., Metha, A.B., Krauskopf, J., Lennie, P., 1999. Rapid adaptation in visual cortex to the structure of images. Science. 285**,** 1405-8.
Nakamura, A., Yamada, T., Goto, A., Kato, T., Ito, K., Abe, Y., Kachi, T., Kakigi, R., 1998. Somatosensory homunculus as drawn by MEG. Neuroimage. 7**,** 377-86.
Nishioka, G.J., Zysset, M.K., Van Sickels, J.E., 1987. Neurosensory disturbance with rigid fixation of the bilateral sagittal split osteotomy. J Oral Maxillofac Surg. 45**,** 20-6.
Nordin, M., Hagbarth, K.E., 1989. Mechanoreceptive units in the human infra-orbital nerve. Acta Physiol Scand. 135**,** 149-61.
Ohzawa, I., Sclar, G., Freeman, R.D., 1982. Contrast gain control in the cat visual cortex. Nature. 298**,** 266-8.
Olausson, H., Wessberg, J., Kakuda, N., 2000. Tactile directional sensibility: peripheral neural mechanisms in man. Brain Res. 866**,** 178-87.
Oldfield, R.C., 1971. The assessment and analysis of handedness: the Edinburgh inventory. Neuropsychologia. 9**,** 97-113.
Padberg, J., Cerkevich, C., Engle, J., Rajan, A.T., Recanzone, G., Kaas, J., Krubitzer, L., 2009. Thalamocortical connections of parietal somatosensory cortical fields in macaque monkeys are highly divergent and convergent. Cereb Cortex. 19**,** 2038-64.
Pantano, P., Formisano, R., Ricci, M., Di Piero, V., Sabatini, U., Barbanti, P., Fiorelli, M., Bozzao, L., Lenzi, G.L., 1995. Prolonged muscular flaccidity after stroke. Morphological and functional brain alterations. Brain. 118 (Pt 5)**,** 1329-38.
Pascual-Marqui, R.D., 2002. Standardized low-resolution brain electromagnetic tomography (sLORETA): technical details. Methods Find Exp Clin Pharmacol. 24 Suppl D**,** 5-12.
Pearce, R.H., Grimmer, B.J., 1972. Age and the chemical constitution of normal human dermis. J Invest Dermatol. 58**,** 347-61.
Peters, R.M., Hackeman, E., Goldreich, D., 2009. Diminutive digits discern delicate details: fingertip size and the sex difference in tactile spatial acuity. J Neurosci. 29**,** 15756-61.
Planetta, P.J., Servos, P., 2008. Somatosensory temporal discrimination learning generalizes to motor interval production. Brain Res. 1233**,** 51-7.
Popescu, E.A., Barlow, S.M., Venkatesan, L., Wang, J., Popescu, M., 2012. Adaptive changes in the neuromagnetic response of the primary and association somatosensory areas following repetitive tactile hand stimulation in humans. Hum Brain Mapp.
Popescu, M., Barlow, S., Popescu, E.A., Estep, M.E., Venkatesan, L., Auer, E.T., Brooks, W.M., 2010. Cutaneous stimulation of the digits and lips evokes responses with different adaptation patterns in primary somatosensory cortex. Neuroimage. 52**,** 1477-86.
Pubols, B.H., Jr., 1982. Factors affecting cutaneous mechanoreceptor response. I. Constant-force versus constant-displacement stimulation. J Neurophysiol. 47**,** 515-29.
Puccini, G.D., Sanchez-Vives, M.V., Compte, A., 2007. Integrated mechanisms of anticipation and rate-of-change computations in cortical circuits. PLoS Comput Biol. 3**,** e82.

Qi, H.X., Lyon, D.C., Kaas, J.H., 2002. Cortical and thalamic connections of the parietal ventral somatosensory area in marmoset monkeys (Callithrix jacchus). J Comp Neurol. 443**,** 168-82.
Rausell, E., Bickford, L., Manger, P.R., Woods, T.M., Jones, E.G., 1998. Extensive divergence and convergence in the thalamocortical projection to monkey somatosensory cortex. J Neurosci. 18**,** 4216-32.
Ridley, R.M., Ettlinger, G., 1976. Impaired tactile learning and retention after removals of the second somatic sensory projection cortex (SII) in the monkey. Brain Res. 109**,** 656-60.
Russo, N., Foxe, J.J., Brandwein, A.B., Altschuler, T., Gomes, H., Molholm, S., 2010. Multisensory processing in children with autism: high-density electrical mapping of auditory-somatosensory integration. Autism Res. 3**,** 253-67.
Sack, A.T., 2009. Parietal cortex and spatial cognition. Behav Brain Res. 202**,** 153-61.
Seitz, R.J., Huang, Y., Knorr, U., Tellmann, L., Herzog, H., Freund, H.J., 1995. Large-scale plasticity of the human motor cortex. Neuroreport. 6**,** 742-4.
Smirnakis, S.M., Berry, M.J., Warland, D.K., Bialek, W., Meister, M., 1997. Adaptation of retinal processing to image contrast and spatial scale. Nature. 386**,** 69-73.
Sperry, R.W., 1950. Neural basis of the spontaneous optokinetic response produced by visual inversion. J Comp Physiol Psychol. 43**,** 482-9.
Spybrook, J., Raudenbush, S.W., Liu, X., Congdon, R., Martinez, A., 2008. Optimal Design for longitudinal and multilevel research: Documentation for the "Optimal Design" software. Vol., W.T.G. Foundation, ed.^eds., New York.
Stal, P., Eriksson, P.O., Eriksson, A., Thornell, L.E., 1987. Enzyme-histochemical differences in fibre-type between the human major and minor zygomatic and the first dorsal interosseus muscles. Arch Oral Biol. 32**,** 833-41.
Stal, P., Eriksson, P.O., Eriksson, A., Thornell, L.E., 1990. Enzyme-histochemical and morphological characteristics of muscle fibre types in the human buccinator and orbicularis oris. Arch Oral Biol. 35**,** 449-58.
Stevens, J.C., Choo, K.K., 1996. Spatial acuity of the body surface over the life span. Somatosens Mot Res. 13**,** 153-66.
Stevens, J.C., Cruz, L.A., 1996. Spatial acuity of touch: ubiquitous decline with aging revealed by repeated threshold testing. Somatosens Mot Res. 13**,** 1-10.
Tannan, V., Whitsel, B.L., Tommerdahl, M.A., 2006. Vibrotactile adaptation enhances spatial localization. Brain Res. 1102**,** 109-16.
Teitelbaum, P., Teitelbaum, O., Nye, J., Fryman, J., Maurer, R.G., 1998. Movement analysis in infancy may be useful for early diagnosis of autism. Proc Natl Acad Sci U S A. 95**,** 13982-7.
Tomberg, C., Desmedt, J.E., Ozaki, I., Nguyen, T.H., Chalklin, V., 1989. Mapping somatosensory evoked potentials to finger stimulation at intervals of 450 to 4000 msec and the issue of habituation when assessing early cognitive components. Electroencephalogr Clin Neurophysiol. 74**,** 347-58.
Trulsson, M., Essick, G.K., 1997. Low-threshold mechanoreceptive afferents in the human lingual nerve. J Neurophysiol. 77**,** 737-48.
Venkatesan, L., Barlow, S., Popescu, M., Popescu, A., Auer, E.T., 2010. TAC-Cell inputs to human hand and lip induce short-term adaptation of the primary somatosensory cortex. Brain Res. 1348**,** 63-70.

Verrillo, R.T., 1979. Change in vibrotactile thresholds as a function of age. Sens Processes. 3**,** 49-59.
Verrillo, R.T., 1980. Age related changes in the sensitivity to vibration. J Gerontol. 35**,** 185-93.
Verrillo, R.T., 1993. The effects of aging on the sense of touch. In Sensory Research: Multimodal Perspectives. Vol., R.T. Verrillo, ed.^eds. Lawrence Erlbau, Hillsdale, NJ, pp. 260-275.
Verrillo, R.T., Bolanowski, S.J., Gescheider, G.A., 2002. Effect of aging on the subjective magnitude of vibration. Somatosens Mot Res. 19**,** 238-44.
Verzar, F., 1963. The aging of collagen. Sci Am. 208**,** 104-14.
Vierck, C.J., Jr., 1974. Tactile movement detection and discrimination following dorsal column lesions in monkeys. Exp Brain Res. 20**,** 331-46.
Vierck, C.J., Jr., Cohen, R.H., Cooper, B.Y., 1983. Effects of spinal tractotomy on spatial sequence recognition in macaques. J Neurosci. 3**,** 280-90.
Vigario, R., Sarela, J., Jousmaki, V., Hamalainen, M., Oja, E., 2000. Independent component approach to the analysis of EEG and MEG recordings. IEEE Trans Biomed Eng. 47**,** 589-93.
Von Holst, E., 1954. Relations between the central nervous system and peripheral organs. British Journal of Animal Behaviour. 2**,** 89-94.
Walter, J.M., Jr., Gregg, J.M., 1979. Analysis of postsurgical neurologic alteration in the trigeminal nerve. J Oral Surg. 37**,** 410-4.
Willis, W.D.,Jr., Coggeshall, R.E., 1991. Sensory Mechanisms of the Spinal Cord. Vol., Plenum, New York, NY.
Wilson, D.A., 1998. Synaptic correlates of odor habituation in the rat anterior piriform cortex. J Neurophysiol. 80**,** 998-1001.
Wittling, R.A., Schweiger, E., Rizhova, L., Vershinina, E.A., Starup, L.B., 2009. A simple method for measuring brain asymmetry in children: application to autism. Behav Res Methods. 41**,** 812-9.
Wohlert, A.B., Smith, A., 1998. Spatiotemporal stability of lip movements in older adult speakers. J Speech Lang Hear Res. 41**,** 41-50.
Wolpert, D.M., Miall, R.C., 1996. Forward Models for Physiological Motor Control. Neural Netw. 9**,** 1265-1279.
Wolpert, D.M., 1997. Computational approaches to motor control. Trends Cogn Sci. 1**,** 209-16.
Wolpert, D.M., Ghahramani, Z., 2000. Computational principles of movement neuroscience. Nat Neurosci. 3 Suppl**,** 1212-7.
Xerri, C., Merzenich, M.M., Peterson, B.E., Jenkins, W., 1998. Plasticity of primary somatosensory cortex paralleling sensorimotor skill recovery from stroke in adult monkeys. J Neurophysiol. 79**,** 2119-48.
Zaytoun, H.S., Jr., Phillips, C., Terry, B.C., 1986. Long-term neurosensory deficits following transoral vertical ramus and sagittal split osteotomies for mandibular prognathism. J Oral Maxillofac Surg. 44**,** 193-6.